CORBETT GEOLOGICAL SERVICES Pty. Ltd.
A.C.N. 002 694 760
6 Oakville Road, Willoughby, N.S.W. 2068, Australia
Phone (+61) (0) 409 306063
E-mail: greg@corbettgeology.com Web: www.corbettgeology.com

COMMENTS ON

THE EXPLORATION POTENTIAL

OF THE

BOTTLETREE PROJECT,

NORTH QUEENSLAND

Greg Corbett
20 March 2023

SUMMARY

The Bottletree porphyry Cu-Mo prospect, Greenvale district North Queensland, was examined in several diamond drill holes from an EW section at Anomaly A and one drill hold form Anomaly B. Zoned hydrothermal alteration and mineralisation within the wall rocks are typical of those currently used as vectors by exploration geologists in the search for blind porphyry Cu-Mo deposits.

Host rocks comprise metamorphosed and deformed metavolcanic and metasedimentary rocks into which have been emplaced dykes with a wide range of overall diorite-tonalite (dacite) compositions, and porphyry textures.

Two structural elements are currently interpreted for Bottletree as:
A penetrative foliation, typical of conditions of ductile deformation formed in association with complex folding and which displays some indication of local development as a multiphase foliation. Alteration minerals such as actinolite form axial planar to folds in the orientation of the foliation, just as this foliation is axial planar to folded epidote veins. Biotite-chalcopyrite alteration is folded by this deformation with a progressively increased mineral alignment. Additional chalcopyrite was introduced during late stage brittle extensional reactivation of the foliation. Overall, much of the Cu mineralisation is controlled by this steep west dipping foliation.
Moderate west dipping normal faults and shears are interpreted to have participated in the development of sigmoid shaped portions of deep epithermal (porphyry D) veins in the eastern portion of the section line, with high Cu contents. These structures are tentatively projected west to have possibly been involved in the emplacement of intrusions and Mo mineralisation, although structural relationships remain unconstrained.

Wall rock hydrothermal alteration displays zonation typical of settings near porphyry heat sources, used as exploration vectors to blind porphyry Cu mineralisation, here with the additional control of the penetrative foliation in both the ductile and brittle regimes. Propylitic-potassic alteration zonation characterised by the indicator minerals: chlorite -> epidote -> actinolite -> biotite, broadly grades, from cool to hot conditions of formation, along the EW drill section east to west and to depth in the west, and is also developed marginal to foliation-related feeder zones. The common wall rock potassic biotite-chalcopyrite assemblage associated with feeder shears lies in a setting close to any speculate porphyry heat source.
Phyllic alteration, best developed in association with porphyry dykes locally overprints and downgrades prograde alteration.

Cu and Mo mineralisation are disconnected in time and space as is recognised in other porphyry deposits. Early Cu is best developed as the prograde biotite-chalcopyrite mineral assemblage during deformation and in foliation partings reactivated during later brittle deformation. It is difficult to estimate the degree of transport from source within these structures. D veins used as exploration vectors towards porphyry source rocks are also well developed with a syn-tectonic relationship to deformation. By contrast the Mo mineralisation displays a high variation in orientations including associated with shears and phyllic altered intrusions. The two metals may be associated with different intrusion sources. The association with phyllic altered dykes suggests Mo is later than Cu.

It is recommended this geological model be applied to the entire tenement with a priority A to prioritise all the existing prospects for further work. The target at the western end of the Anomaly A is currently provided with a priority AB, as although highly prospective, it remains unknown how deep the target may lie below the deepest drill intercept of 750m below surface. The planned review should place this analysis of the EW drill section at Anomaly A in a context and may change the priority ranking. Anomaly B contains dominantly epidote wall rock alteration, formed more distal to the heat source than the alteration in anomaly A and so is provided with a priority B. Some age dates would contribute towards the Bottletree geological model.

INTRODUCTION

A total of 8 days were spent in at the Terra Search exploration facility in Townsville (27-30 August 2022 and 6-10 February 2023) in a review of drill core from mainly one EW section at Target A of the Bottletree Prospect (figure 1), while one drill hole from target B was also considered. No field inspection was included. Initially this review sought to address the question posed by Ian Kelso - "is this porphyry Cu mineralisation" and provided a preliminary analysis of the zoned alteration. Later, that study was updated (herein) with the analysis of DDH BTDD010 bored after the initial inspection. This geological model, that includes many assumptions, for an unusual and complex wall rock hosted porphyry alteration and mineralisation system, is expected to further evolve as additional field data comes to hand. The assistance is greatly appreciated in this work of Superior Resources Limited geologists, Peter Hwang, Ian Kelso and Peter Gregory as well as Terra Search staff Simon and Tim Beams, Travers Davies, Ben Hoffman and others.

Priority

Exploration projects are rated with priorities to proceed with the planned work program to take them to the next decision point. Any such a grading might include a number of projects at widely differing stages of evaluation, some with substantial data bases, while others might be unexplored, but may display considerable untested potential. Priorities are based upon the data to hand at the time of inspection, and are subject to change as increased exploration provides improved and additional data. Projects are categorised as:

A – Of highest interest such that the proposed exploration program should be carried out immediately. However, early-stage projects with untested potential might be rapidly down graded from this stage by completion of the planned work program.

B – Of some interest and should be subject to further work if funds are available, often with smaller components of continued exploration expenditure than higher priority targets.

C – Of only little interest and subject to further work at a low priority if funds are available, but not to be relinquished at this stage.

D – Of no further interest and can be offered for joint venture or relinquished.

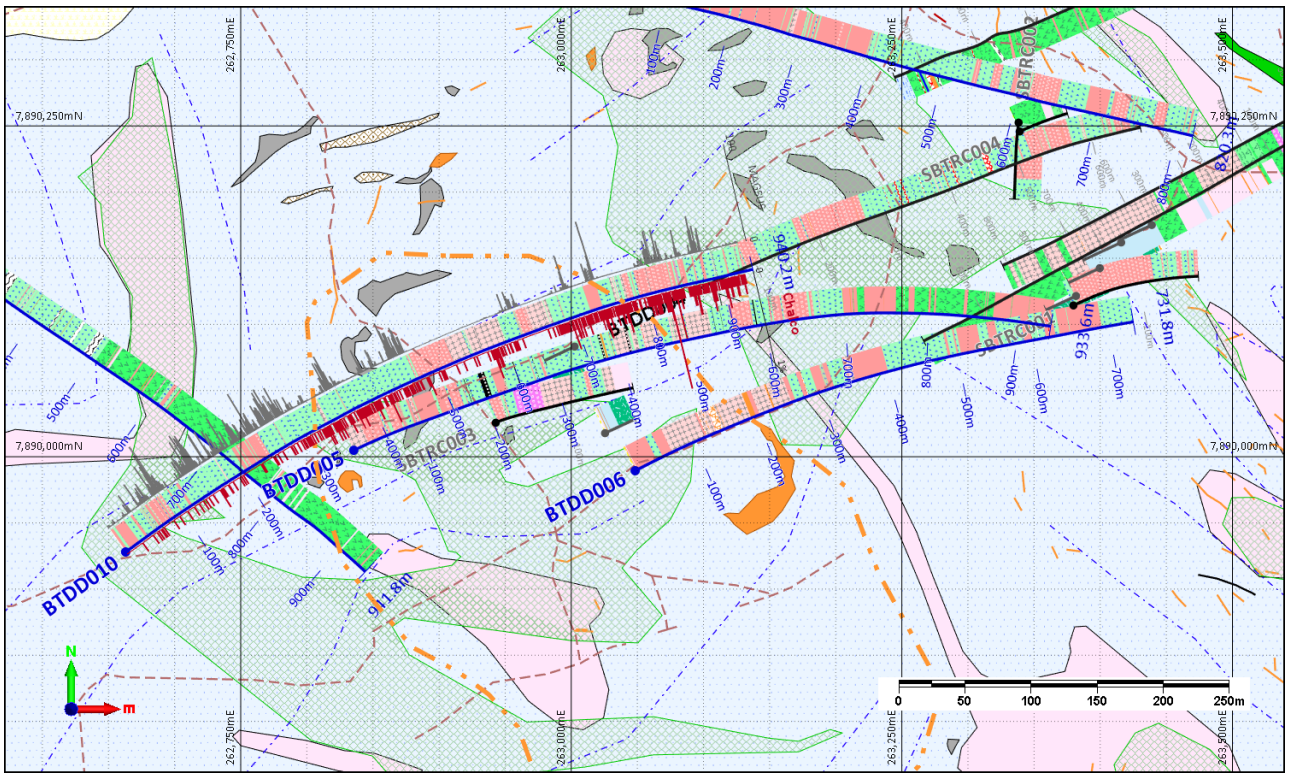

Figure 1 Location of the drill holes partly inspected in this review as, BTDD001, 4, 5, and 10 which constitute the majority of this review, inlcuded as the section in figure 4, Superior Resources data.

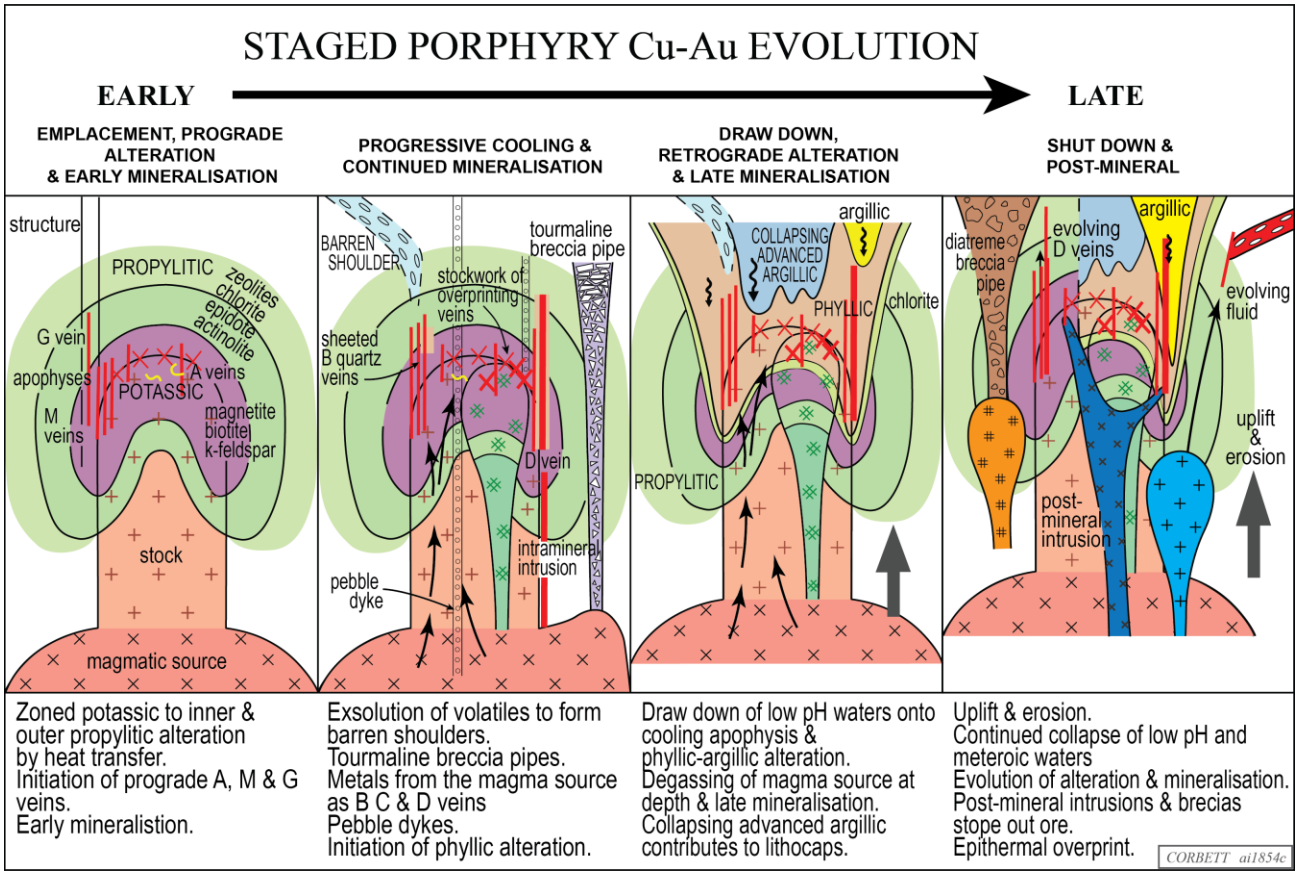

Figure 2. Progressive development of porphyry Cu-Au deposits, from Corbett (2019) and updates. Prograde hydrothermal alteration zonation within the wall rocks, shown at the far left, is of greatest interest here as an out of porphyry vector towards blind porphyry Cu mineralisation.

Methodology

In answer to the question posed by Ian Kelso, the mineralised veins and wall rock hydrothermal alteration recognised in the Bottletree drill core are porphyry-related and typical of features commonly recognised within the wall rocks outside mineralised porphyry Cu $\pm$Au $\pm$ Mo intrusions. *Out of porphyry* features in the wall rocks are used as exploration vectors towards blind porphyry Cu ($\pm$Au $\pm$ Mo) mineralisation. In some other instances, these wall rock veins form economic "wallrock porphyry" Cu-Au-Mo deposits (Cadia district), developed above buried magmatic source rocks for mineralisation.

The geological model used herein (Corbett and Leach, 1998; Corbett, 2019 & in prep) suggests porphyry Cu intrusions develop at the apophysis of buried batholitic intrusive source rocks for the polyphasal intrusions that make up the porphyry and also metals which enter the porphyry environment as the buried magmatic source cools. Porphyry Cu deposits typically develop within magmatic arcs at collisional tectonic plate boundaries, manifest as compressional kinematic settings. However, many porphyry and epithermal Cu-Au deposits display kinematic conditions of mineralised vein formation at odds with the regional tectonism, developed as an indication spine-like vertically attenuated porphyry intrusions have been forcefully emplaced into wall rocks during transient changes from compressive to extensional tectonism and this dilatant structural environment then facilitates migration of ore fluids from the magmatic source to the overlying intrusion.

Consequently, the focus of this study has been to use *out of porphyry* features (hydrothermal alteration, veins, dykes & breccias) as vectors towards blind buried porphyry Cu mineralisation. While mineralised veins are of use, the main vector employed at Bottletree has been zoned prograde

wall rock hydrothermal alteration. Models for porphyry Cu mineralisation (figures 2-4; Corbett and Leach, 1998; Corbett, 2019 & in prep) suggest the earliest stage of porphyry emplacement prograde hydrothermal alteration of the wall rocks is zoned outward from the cooling hot intrusion from potassic (biotite, Kfeldspar, magnetite), to inner propylitic (actinolite, albite, adularia) and outer propylitic (chlorite, carbonate) alteration, governed by well-defined conditions for the formation of individual minerals (figures 2-4). This study seeks to trace this zoned hydrothermal alteration down towards a targeted heat source (stage 1 in figure 2). Later phyllic (silica-sericite-pyrite) alteration which commonly overprints and destroys the prograde hydrothermal alteration (stage 3 in figure 2) is noted but of little use in this analysis. Many mineralised veins are likened to D veins typical of those developed in the wall rocks in the vicinity of porphyry Cu intrusions.

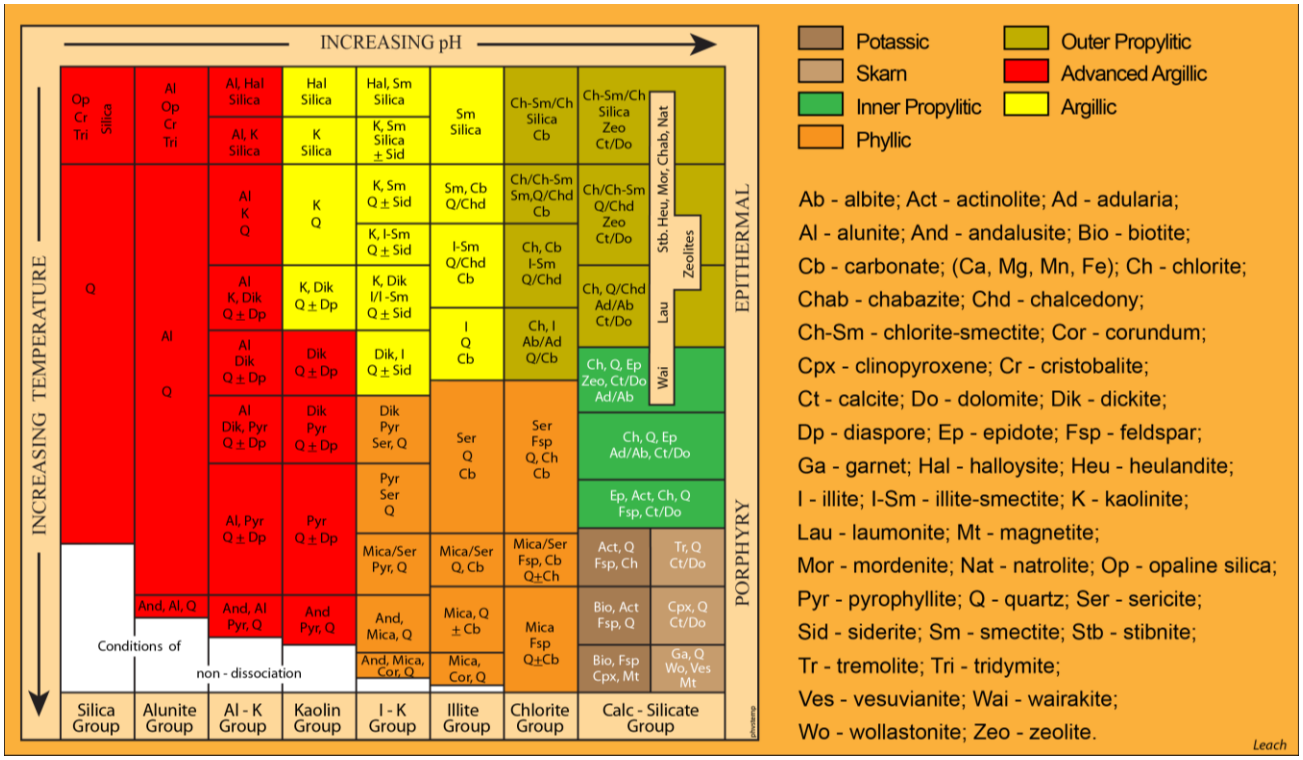

Figure 3 Zonation in alteration minerals in porphyry-epithermal deposits (from Corbett and Leach, 1998 and discussed in updates).

APPLICATION TO BOTTLETREE

At Bottletree *out of porphyry* features typically recognised in wall rocks near porphyry Cu intrusions display a strong association with a penetrative foliation rather than brittle fractures typical most porphyry Cu deposits. Such foliations and folded rocks typically develop at deep crustal levels in conditions of ductile deformation below the brittle-ductile transition, commonly estimated as greater than 10-20km depth, depending upon many factors derived from experimental data. By contrast porphyry Cu deposits typically develop at significantly shallower crustal levels in conditions of brittle deformation. The vertically attenuated spine-like polyphasal intrusions such as at the Goonumbla and Ridgeway porphyry Cu-Au deposits, Australia, may rise to depths as shallow as 2km, while the stock-like porphyry intrusion such as Bingham Canyon, considered to be a typical porphyry Cu deposit, tops-out at 3-5 km depth (Porter et al., 2012), and some of the deepest porphyry mineralisation at Butte, Montana, is estimated to have been emplaced at depths of 7-8km (Rusk et al., 2008). The Yerrington, Nevada, porphyry system is turned on its side and eroded to expose an original porphyry anatomy to the batholitic magmatic source at 7 km depth (Dilles et al., 2000).

The ductile deformation at Bottletree it interpreted herein to have resulted from the coincidence of high temperatures, derived from the buried magmatic source, and localised high strain, in an environment sealed by hydrothermal alteration to restrict access of meteoric waters. Fournier (1999) describes examples of the brittle-ductile transition in other porphyry systems and goes on to suggest fluids may undergo considerable vertical transport in conditions of brittle failure. At Bottletree, there is some suggestion of a transition from ductile to brittle condition as the foliation, developed during initial hydrothermal alteration and mineralisation, was subsequently reopened to receive additional sulphide mineralisation in brittle conditions (below, photos 7, 8 & 24), possibly during transient changes to extensional stress conditions. This is consistent with the paragenetic sequence of porphyry alteration and mineralisation (figure 2).

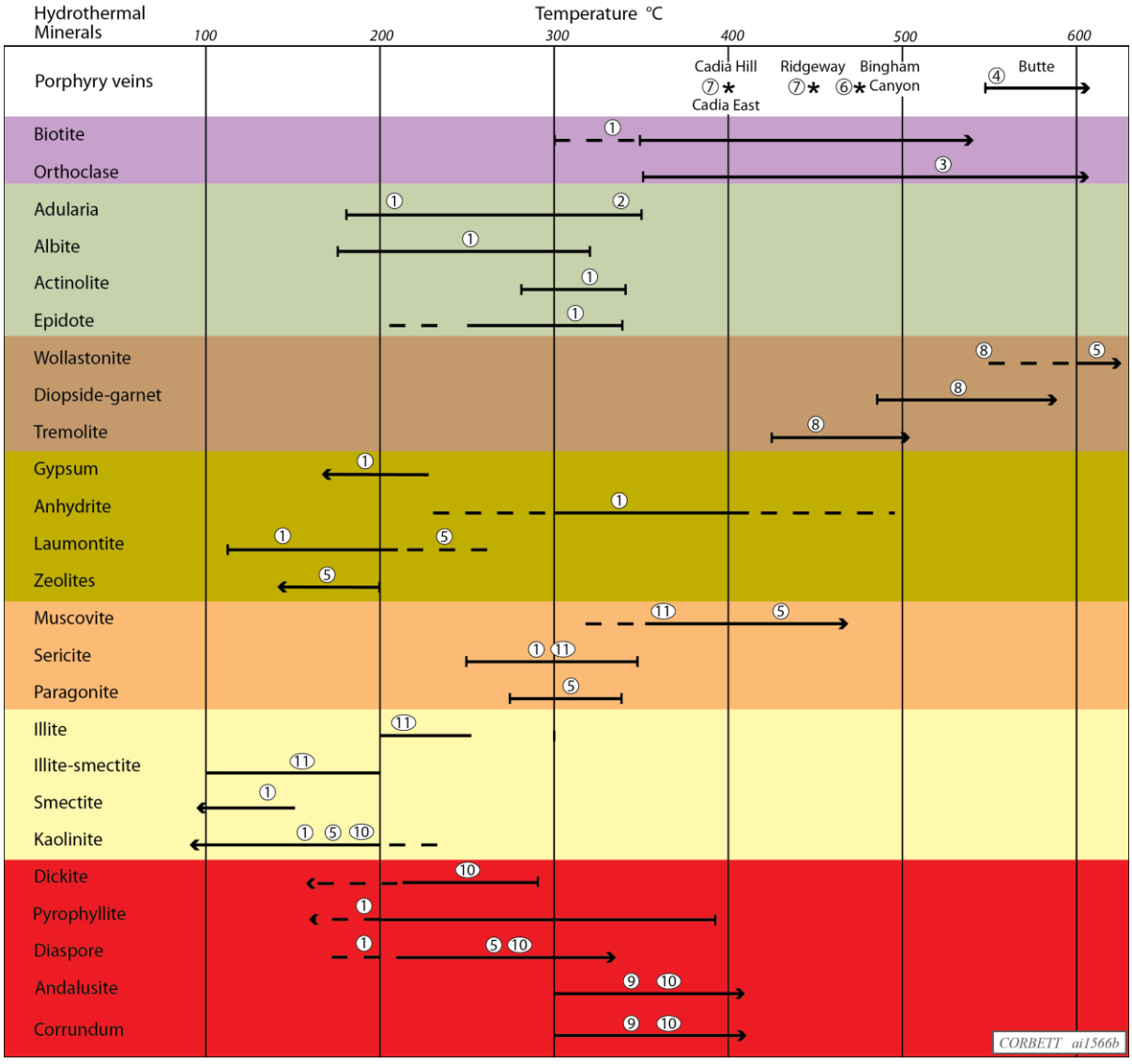

Figure 4 Formation temperature of common alteration minerals (from Corbett short course notes).

Geological setting

The Bottletree district lies about 215 km west of Townsville, North Queensland, hosted within the Cambro-Ordovician Eland Metamorphics of the Greenvale Provence (Henderson and Withnall, 2013) described as chlorite-albite shist with additional quartz, actinolite, carbonate and epidote, all minerals formed in conditions of low grade metamorphism as well as propylitic hydrothermal alteration. Detailed mapping (Tate, 2021) suggests the Bottletree geology is dominated by metamorphosed equivalents of volcanic and sedimentary rocks as well as dioritic intrusions with propylitic and phyllic hydrothermal alteration typical of magmatic arcs. Tate (op cit) suggests the

diorites are similar to others marginal to Bottletree to the Ordovician Lynwater Complex, and there are similarities between his quartz-magnetite rocks to skarnoid recognised in DDH BTDD007 70-85m and his buck quartz veins and gossanous breccias to porphyry D veins and lodes. This study evaluates Bottletree as a more metamorphosed equivalent of Tasmanide magmatic arcs of a possible similar age to the south, although continued exploration should seek to enhance the understanding of the geological context.

ANOMALY A
Host rocks

Wall rocks in drill core are dominated by strongly metamorphosed and deformed andesitic volcanics and pelitic sediments (below) into which have been emplaced a variety of dykes with common porphyritic textures, which vary from cm scale to several tens of metres in width, and are dominated by diorite, tonalite (dacite) compositions. The dykes therefore display considerable variation in texture, composition and alteration. This exercise categorised at least five different diorite variants and also dacite in the 550-600m interval of BTDD010. Most dykes are aligned within the foliation and display some deformation. Some dykes (below) are interpreted to have been emplaced into structural zones and undergone later molybdenite mineralisation. By contrast, narrow undeformed molybdenite-bearing aplite dykes in the drill intercept DDH DTDD005 420-525m (photo 1) cross cut the foliation and so are taken to be late and could be related to the event of Mo mineralisation that cuts earlier dykes. While some dykes are fresh, the primary mafic minerals are overprinted by secondary biotite (photo 2) of potassic alteration and many display weak to intense sericite of phyllic alteration (photo 3). The abundant molybdenite at the margins of phyllic altered dykes at about 474m in DDH BTDD010 (photo 3) is assumed to have been emplaced following dyke emplacement. Therefore, the variety of dykes may occupy a range from pre-, to syn- and post-mineral emplacement and display a relationship with speculated structures.

Structure

Two structural elements appear to control the development of alteration and Cu-Mo mineralisation discernible in drill core for the EW section at Bottletree Anomaly A.

The penetrative foliation forms the principal metamorphic fabric in the wall rocks discernible in drill core varying from a slaty cleavage (photo 4-5) with prograde and minor retrograde hydrothermal alteration, to a phyllitic character, which with increasing deformation and local alteration, progressively becomes more commonly differentiated to a fabric with M (micaceous) and QF (quartzofeldspathic) domains (photos 6-8). It is the product of polyphasal deformation, evidenced by dismembered or marooned fold hinges (photo 9), and displays a relatively consistent 60^{o} west orientation cutting most rock types, although some dykes might exploit the foliation late deformation (photo 23). The rock sequence displays considerable folding. Hydrothermal alteration minerals are aligned within the foliation, including as axial planar to folds, such as epidote (photo 14-15), actinolite (photos 11 & 13) and biotite (photos 2, 5. 11-13) as well as sulphides, typically pyrite-chalcopyrite (photo 7-8) and within veins and shears (below). Some sulphides appear to fill reopened partings on the foliation (photos 7-8). There are many examples of folded hydrothermal mineral veins (epidote, photos 14-15; biotite, photo 21) as well as early massive quartz veins likened to porphyry A veins which cut the foliation, and aligned with the foliation axial planar to small scale folds (photos 16-17). Similarly, common bands of folded hydrothermal alteration may reflect preferential replacement of favourable lithologies and/or fluid channelways (photos 18-20). Many of these folds display development of axial planar hydrothermal minerals (photos 20-21). The highset temperature alteration minerals such as biotite (photos 12-13, 21-22) display a common control in high strain zones which cross-cut lower temperature alteration such as chlorite and the biotite alteration locally grades to lower temperature actinolite in the adjacent wall rocks. Many dykes (photo 23), veins (photo 24), and alteration minerals are aligned within the foliation,

commonly introduced later. The important biotite-chalcopyrite mineralisation is typically aligned within the foliation (photos 11-12 & 30) as are quartz sulphides, some likened to D veins (photo 24) and many display continued deformation (photos 25-30). The foliation planes have been reactivated to host chalcopyrite mineralisation varying from thin stringers (photos 7-8), to shears in which the foliation has been reactivated (photos 28-29). Importantly, the biotite-chalcopyrite mineral assemblage is typically aligned within the foliation (photos 17 & 30-31) as continued activation reorients initially random chalcopyrite stringers (photo 17) into the foliation (photo 30). Only in rare instances is foliation cut and offset by later chalcopyrite mineralisation

Therefore, it is proposed alteration began at the same time as deformation such that bands of alteration are folded and also contain axial planar alteration minerals and sulphides exploit the foliation. Veins exploit the foliation and are folded by it. Models for porphyry Cu mineralisation (Corbett, 2019; figure 2) feature the introduction of some mineralisation with intrusion emplacement and alteration, followed by continued Cu mineralisation after that alteration, as the magmatic source at depth cools and degasses.

Interpreted moderate west-dipping shears might also influence the trend of mineralisation, although the orientation is poorly constrained at this time. Analysis by Superior Resources suggests the penetrative foliation trends roughly NS (at right angles to the section line) and dips about 60-70^{o} west (figure 6), at a high angle to the east-trending drill holes at the western end of the section line. However, the west-trending drill holes at the eastern end of the section line (SBTRD006 and BTDD001) are bored parallel to the foliation. Where identified in these drill holes the core-parallel mineralised deep low sulphidation epithermal (quartz-pyrite-pyrrhotite-chalcopyrite) or D veins, form thick portions at the centre of sigmoids which terminate in shears at a low angle to the core axis (photos 32-35). Deeper crustal level quartz-sulphide Au veins tend to host chalcopyrite and pyrrhotite (photos 34-35). A model using Bottletree oriented drill core and comparisons with similar features elsewhere (Drake, Australia; Palmarejo, Mexico; Corbett, unpubl. data) suggests normal-fault movement on moderate west-dipping normal faults/shears facilitated the formation of sigmoid vein portions (figure 5) and therefore provide an irregular distribution to mineralisation.

Moderate west dipping normal faults appear to also penetrate western Bottletree cutting the earlier foliation and associated with mineralisation. In DDH BT004 the typical biotite-chalcopyrite within the foliation at a moderate angle to the core axis (photo 31) passes at shears about 360m downhole to foliation-parallel sigmoidal quartz-pyrite-pyrrhotite-chalcopyrite veins to a major structure at 525m (figures 5 & 6; photo 34). Although this drill hole trends to the west the foliation appears to have been reoriented and now lies parallel to the core axis in the interval of the sigmoids and therefore reoriented from the general foliation orientation. The major structure at 525m hosts pyrite-chalcopyrite with 0.12 ppm Au and 0.6% Cu likened to quartz-sulphide Au $\pm$ Cu low sulphidation epithermal mineralisation (photo 36). Another major structure towards the end of hole hosts 6m @ 0.8% Cu within folded foliation (photos 37-39) at 631-637m (figure 6).

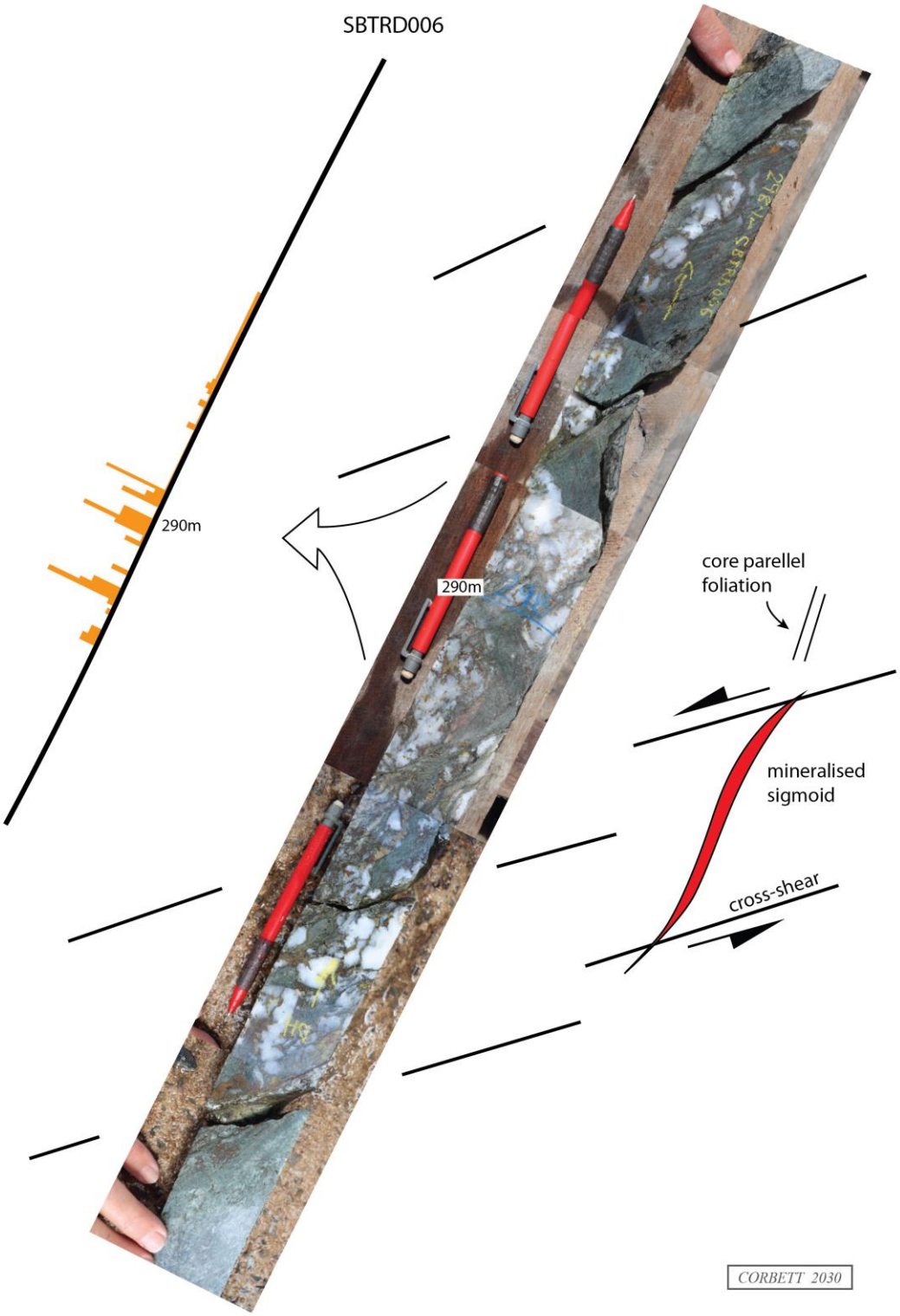

Figure 5 Interpretation of typical sigmoid in drill core with Au histogram on the left hand side.

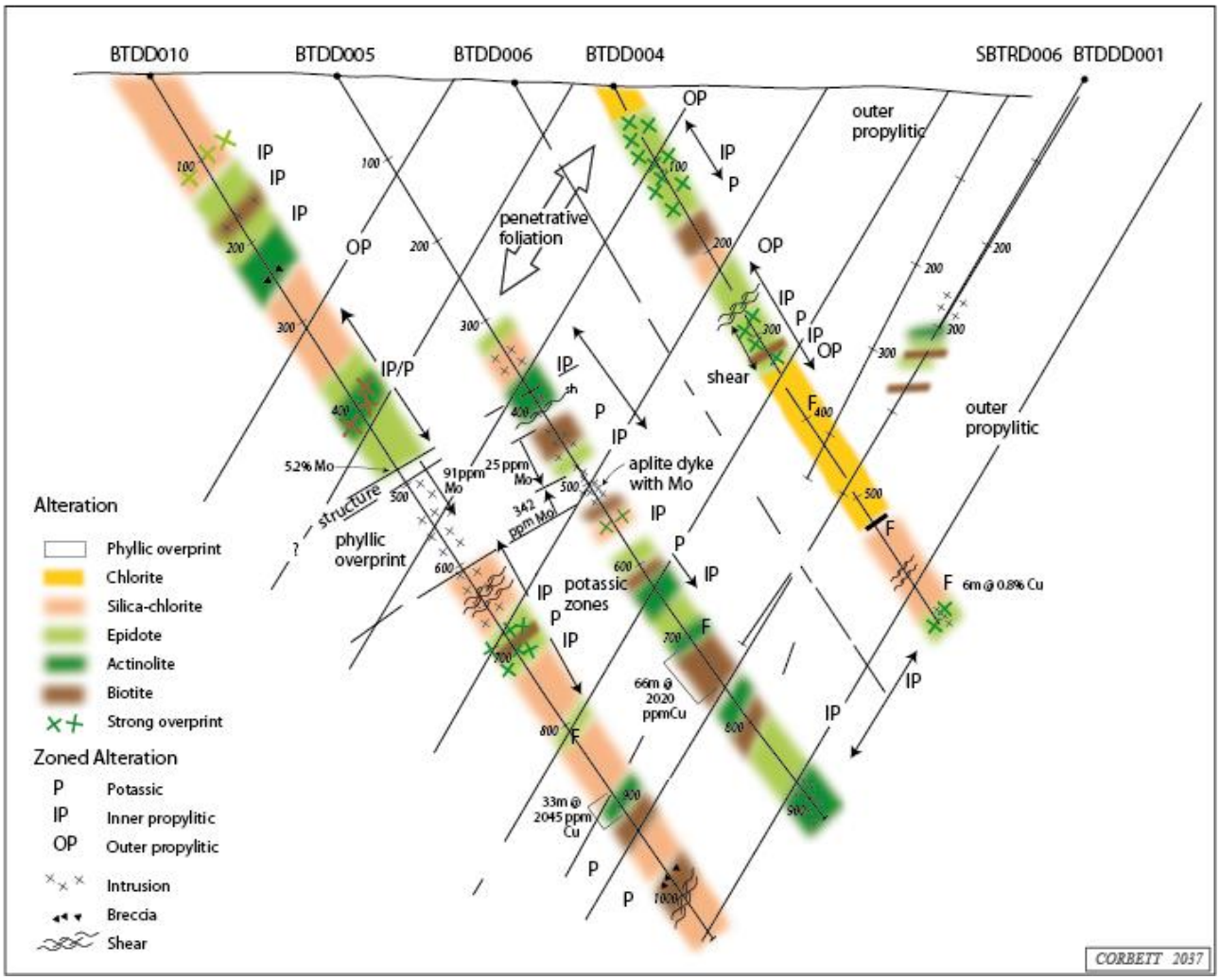

Figure 6 The EW drill section at Bottletree showing hydrothermal alteration, structure and mineralisation on the drill holes inspected to date.

The Upper Mo Zone is defined by the abundance of interpreted mostly epigenetic Mo mineralisation hosted within many different diorite-dacite intrusions which display alteration varying from biotite to intense phyllic overprints (figure 6). Only minor Mo mineralisation, such as in the Mo-bearing aplitic dykes (photo 1) is interpreted to lie within source intrusions as disseminations and stringers. The source of the Mo dykes remains unknown, but may be the same as the epigenetic Mo which is hosted in older dykes. While the moderate west-dipping faults noted in the eastern portion of the anomaly A section have been projected to the west as an overall control the intrusion emplacement, much of epigenetic Mo mineralisation appears to be aligned within the penetrative foliation. Superior Resources data provides a wide spread for the orientation of the Mo mineralisation, including with many flat dipping fracture/veins, in contrast to the Cu mineralisation which is aligned in the foliation. The most striking portion of the Mo Zone is the 5.2% Mo at 474min DDH BTDD010 (photo 3), which continued downhole to 540m as 66m @ 91ppm Mo and terminates downhole at a sheared contact with Cu mineralised (16m @515ppm Cu) and barren dacite intrusions to 600m.

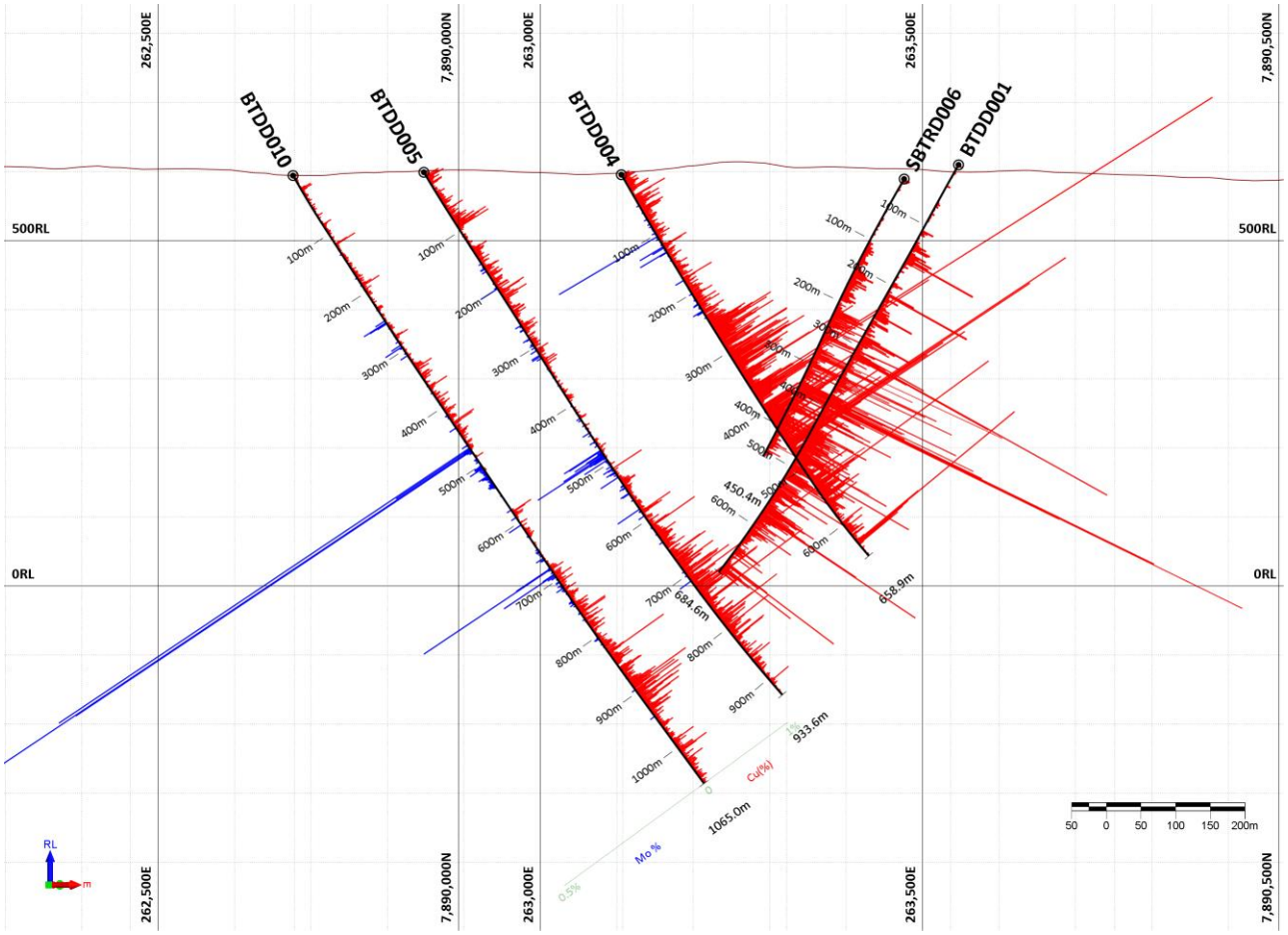

Figure 7 Assay data as histograms for the EW section at Anomaly A (Superior Resources Data).

In DDH BT005 biotite-altered tonalite dykes, with variable sericite overprint, abound from about 400m downhole with patchy Mo anomalism, which rises to 58m @ 25ppm Mo in the 418-476m interval. From 476m downhole the similar dykes host stringer (photo 40) and vein (photo 41) Mo-mineralisation for 34m @ 343ppm Mo. At the base of this zone, dykes which overprint the biotite include a cross-cutting aplite with visible molybdenite mineralisation at 510m (photo 1). These dykes display weak chlorite-sericite alteration and are undeformed and therefore appear to have been emplaced after the epigenetic mineralisation. Deformation increases dramatically downhole from the aplite dykes as patchy Mo mineralisation dominates in deformed quartz veins. This Upper Mo Zone in DDH's BTDD005 and 10 projects east to in DDH BTDD006 as 7m @ 763ppm Mo at 276m and then further east to DDH BTDD004 as 3m @ 230ppm Mo from 229m and 5m @ 25ppm Mo from 239m in (figure 6). Although the trend is discernible, Mo grade declines moving west to east.

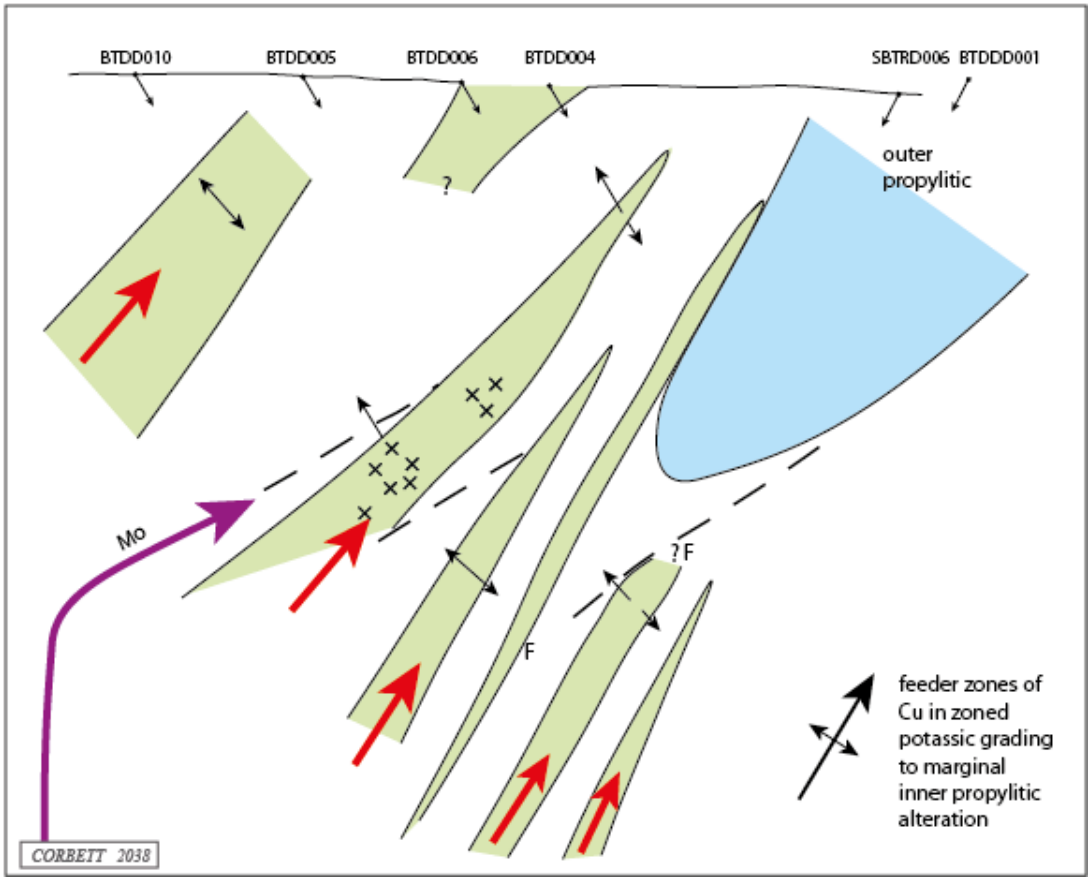

Figure 8 Interpretation of figure 6 showing the interpreted Cu and Mo feeder zones.

Hydrothermal alteration

As noted above, the influence at Bottletree of foliation upon porphyry alteration is unique in this author's experience. While at Bottletree shells of prograde propylitic to potassic hydrothermal alteration that normally indicate increased temperature of hydrothermal alteration towards the intrusion heat source are discernible as broad pervasive alteration, there is also a strong control within the foliation and other structures. In many instances zones of structurally controlled higher temperature biotite (potassic) alteration grades outwards in hand specimen, or over a few metres, to lower temperature actinolite and then epidote alteration and more marginal silica-chlorite. Adularia and less commonly albite may occur with actinolite as a typical propylitic mineral assemblage.

The Lower Mo Zone at DDH BTDD010, 680m hosts 2m @ 2791ppm Mo as part of 17m @ 497m Mo within a shear/breccia zone at a dyke margin as deformed foliation-controls quartz-molybdenite veins (photo 46). This zone can be projected to 195ppm Mo within a diorite dyke at DDH BTDD005, 592m and onwards to 38ppm Mo within a milled breccia at DDH BTDD004, 401m (figure 6).

Nevertheless, there is a broad trend of increased temperature of the hydrothermal alteration indicated by the presence of secondary biotite moving from east to west and to deeper levels (figure 6). The broad zonation is mirrored by a trend from some deep epithermal vein mineralisation (quartz-pyrite-chalcopyrite-pyrrhotite veins) in the east, the potassic biotite-chalcopyrite mineral assemblage to the west increasing at depth. Importantly, the potassic biotite-chalcopyrite assemblage dominates as the Bottletree Cu mineralisation. Exploration therefore seeks to trace the hydrothermal alteration in the wall rocks from low temperature propylitic to higher temperature potassic alteration in an attempt to identify blind porphyry style intrusion at depth using the classification at Bottletree including itallics to identify the critical minerals for the definition of alteration zones in figure 6:

DISTAL TO HEAT SOURCE

Fresh
Green weakly chloritized andesitic volcanic rocks

Outer propylitic alteration

Chlorite-carbonate (photo 9 & 56)

Silica-chlorite (photo 6-10, 16, 27, 32-39, 42, 44)

Silica-chlorite ± adularia as low temperature Kfeldspar (photos 52-53).

Inner propylitic alteration

Silica-chlorite-*epidote* (photos 14, 15, 16, 20, 49)

Silica-chlorite-epidote-*actinolite* ± adularia ± albite (photos 4, 13, 20, 46-49)

Potassic alteration
Secondary biotite ± Kfeldspar (photos 2, 5, 12, 13, 17, 18, 20, 21, 22, 28, 30, 31, 44, 45)

PROXIMAL TO HEAT SOURCE

Biotite is recognised within tonalite-diorite intrusion dykes (photos 2, 5) and bands in the wall rocks mostly controlled by foliation (photos 11-13) with a possible influence by lithology (photo 17-18). Actinolite is recognised within dykes (photo 23), as a pervasive wall rock alteration (photos 1, 48-51), and within the foliation (4, 11, 13), including as axial planar to folds (photo 19-20). Epidote is best developed as veins cross-cutting (photos 14-15) or parallel (photos 10, 16, 51) to the foliation commonly overprinting silica-chlorite or locally in association with actinolite.

Much of the porphyry-style hydrothermal alteration of the metavolcanic and metasedimentary wall rocks is localised within bands, commonly featuring the biotite-chalcopyrite assemblage (figure 6), which may grade to marginal actinolite and epidote in scales ranging from hand specimen or over several metres (photos 18-20). Alteration may parallel foliation within bands which are folded suggesting an early initiation for alteration, and is aligned within the foliation and cross-cuts it. Epidote-actinolite appear to be aligned axial planar to folds (photos 10-11). Folded epidote veins (photos 14-15) and local biotite (photos 11-13) lie within the foliation, and also cross-cut it to be folded with the foliation as axial planar to those folds. What appear to be porphyry A veins are also folded by those folds (photos 7 & 14). Alteration, deformation and Cu mineralisation are regarded as synchronous.

There are numerous instances of locally zone hydrothermal alteration in hand specimen and varying over several metres of zonation from central biotite in possible feeder zones, outwards to actinolite and more marginal epidote-adularia (figure 4). Therefore, the wall rock potassic-propylitic alteration might also be considered as many smaller zones which overall grade out to the averaged alteration depicted in August 2022. The more common association of Kfeldspar with actinolite-epidote, rather than with biotite suggests the Kfeldspar may be the lower temperature form as adularia, rather than higher temperature orthoclase. They are difficult to distinguish optically in the field.

Phyllic alteration dominated by sericite with variable pyrite, chlorite and silica, overprints fresh intrusions and potassic-propylitic alteration, as broad zones of pervasive alteration, typically within the intrusive rocks, and as selvages to veins, as is typical of porphyry-style alteration. As the earlier zoned prograde alteration is of interest here as an exploration vector, the phyllic alteration overprint is not considered in detail (figure 6).

The association of chalcopyrite with secondary biotite (potassic alteration) and molybdenite with sericite (phyllic alteration) which is typically later, contributes to the distinction of two mineralising events and date the molybdenite as later.

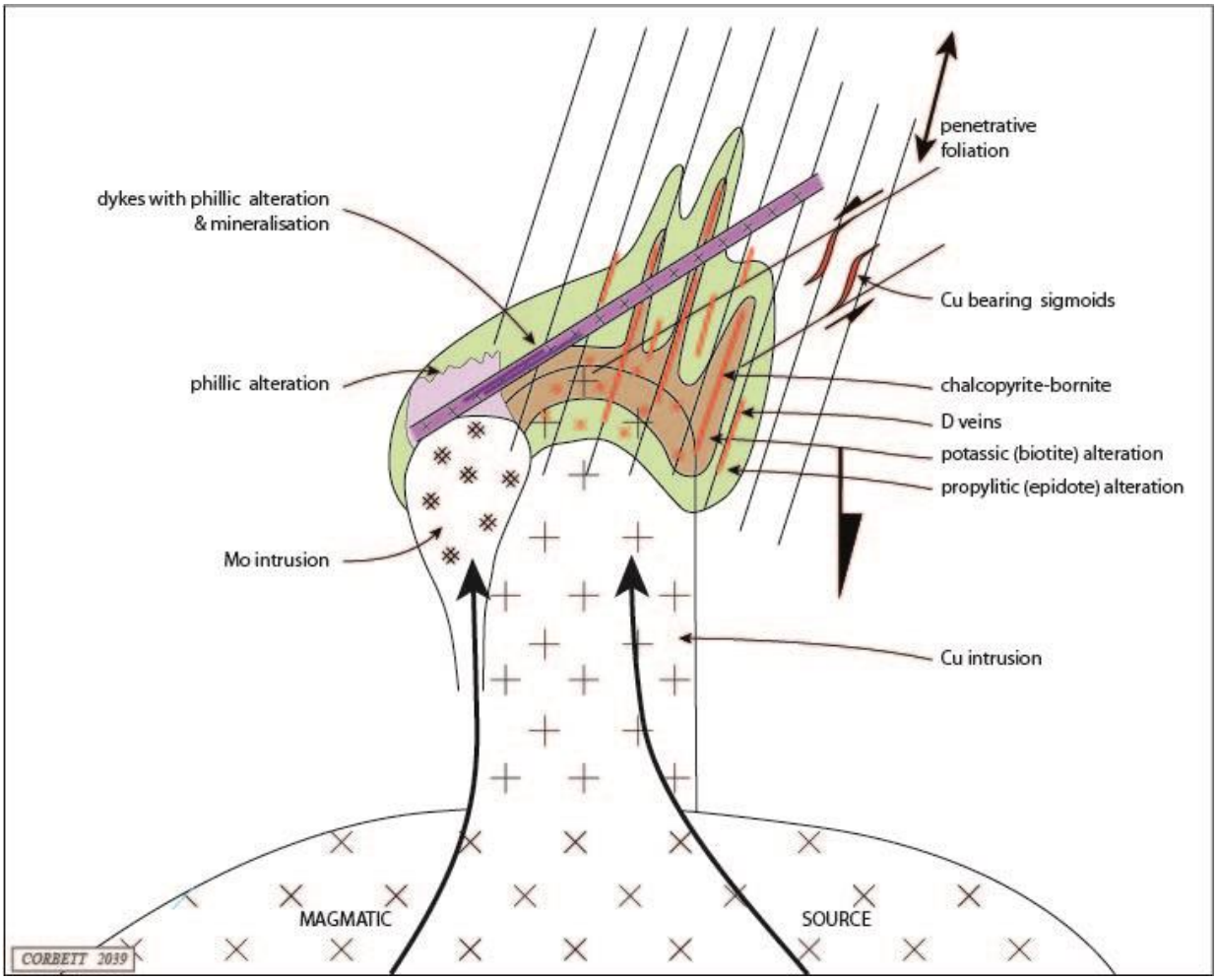

Figure 9 Conceptual model for the Bottletree prospect form the data to hand as at March 2023.

Mineralisation

The mineralisation recognised to date in the Bottletree drill holes inspected is typical of what might be expected within the wall rocks in the vicinity porphyry Cu-Mo style deposits or the magmatic source, albeit with the influence of the foliation. Locally this mineralisation may attain economic wallrock porphyry style such as at the Cadia district. Wall rock hosted veins, dykes breccias and alteration are all *out of porphyry* features used as exploration vectors towards blind porphyry intrusions (Corbett, 2019).

At Bottletree chalcopyrite and molybdenite mineralisation are not linked, but separated spatially and possibly temporally. Virtually no typical porphyry-style chalcopyrite-molybdenite veins were recognised, but only separate Mo and Cu mineralisation are recognised. Both tend to occur in shears, Mo mostly in phyllic altered intrusions (photo 3) and chalcopyrite in company with biotite (photos 12, 17, 30, 44-45), porphyry D style quartz veins (photos 24-26 and shears (photos 27-29)

as well as faults (photos 36-37). Superior Resources has identified different trends for Cu and Mo veins. The Cu mineralisation, as biotite-chalcopyrite and B veins, displays a strong association with the penetrative foliation. By contrast the Mo structures display a wide scatter including flatter orientations. This separation of Cu (with Au) from Mo is common in porphyry Cu-Mo deposits. In several porphyry deposits (Bingham Canyon and Butte, USA) the disconnect between Mo and Cu has been attributed to the earlier deposition of Mo at a higher temperature, and therefore often deeper, than Cu (Seo et al., 2012; Rusk et al., 2008; Porter et al., 2012). Mo anomalism surrounds many porphyry Cu-Au deposits as a shell (Caspiche, Chile; Batu Hijau, Indonesia; Bajo del la Alumbrera, Argentina) and at El Teniente, Chile, is taken to be late (Spencer et al., 2015). In cases where marginal Mo lies within D veins it is regarded as late, as per the paragenetic sequence presented in figure 2. At Bottletree the chalcopyrite-biotite association with potassic alteration is regarded as early whereas molybdenite is best developed cross-cutting retrograde sericite altered dykes is late. Therefore, Cu and Mo appear to display different controls to mineralisation and provide vectors towards possible different intrusion targets.

Copper mineralisation occurs as:

- The biotite-chalcopyrite assemblage represents an important *out of porphyry* mineralisation style developed a part of the potassic alteration and initiated during ductile deformation as it is locally folded (photo 18) and occurs in bands (photo 17) in which the chalcopyrite becomes progressively aligned in the trend of the foliation (photo 30) that is also exploited by sulphide mineralisation (photo 30).
- The foliation was dilated in the brittle regime to host additional chalcopyrite-pyrite along partings (photos 7 & 8) as well as porphyry A and D style veins (photos 24-30). Note some foliation-parallel quartz-chalcopyrite±pyrrhotite vein/breccias without sericite selvages are locally associated with biotite alteration (photo 24-25, 27) or others with sericite alteration selvages which resemble D veins (photo 26).
- Some quartz-chalcopyrite±pyrrhotite veins are likened to deep low sulphidation epithermal and are best developed east of the main porphyry-related biotite alteration, locally overprinting porphyry alteration and mineralisation (photos 32-35).
- There is a decline in temperature in the EW section from porphyry in the west to epithermal in the east.
- Chalcopyrite is also localised within fault zones such as the footwall fault in DDH BTDD004 (6m @ 0.12ppm Au and 0.8% Cu) where it infills the folded foliation and is assumed to be coeval with folding, but may have filled open space later (photos 37-39). A fault zone in the same drill hole (photo 36) resembles deep low sulphidation quartz-sulphide Au±Cu mineralisation (Corbett and Leach, 1998; Corbett, 2013)
- Possible bornite was recognised in another fault zone (photo 27) as a transition to later and distal lower pH conditions, although it must be verified whether this bornite is a tarnish to chalcopyrite.

Molybdenite mineralisation occurs as:

- Substantial molybdenite fills dyke-hosted factures at the margins of structural zones and is considered to post-date those phyllic altered dykes derived from a deeper magmatic source (photo 3).
- Rare molybdenite-bearing aplite dykes (photo 1) might also be linked to the magmatic source for mineralisation.
- Locally sheared veins are likened to D veins as quartz-molybdenite localised within the foliation and with selvages of sericite alteration (photo 46).
- One solitary porphyry-style quartz-molybdenite vein with a prograde epidote selvage cuts the foliation and is cut by it, and so represents syn-deformational porphyry-related prograde Mo mineralisation recognised only in the top of DDH BTDD010 at the extreme west of the EW section (photo 54).

ANOMALY B

One drill hole at anomaly B, DDH BTDD007, was briefly examined in as a comparison to anomaly A.

Host rocks are similar as strongly foliated metavolcanics and lesser sediments with local intrusions, such as the phyllic altered hornblende diorite porphyry in the 55-66m interval, which contained a maximum Cu content of at 59-59m of 420 ppm Cu. No gold is associated with red sphalerite at 57-58m, although it is indicative of an elevated epithermal temperature of formation, but well below that of porphyry mineralisation.

Hydrothermal alteration of the chloritic metavolcanic rocks varies from lowest tenure outer propylitic chlorite-carbonate (photos 9 & 56) to silica-chlorite flooding (photo 6) and epidote (photos 15, 57 & 60) with local adularia (photo 55). Epidote, as flooding, disseminated, vein shear forms, is the most distinctive mineral, although minor actinolite (photo 56) is also present. Consequently, wall rock alteration might be placed in figures 2-4 as mostly in the lower temperature portion of inner propylitic alteration characterised by an epidote overprint on chlorite. Insufficient actinolite is present to consider the higher temperature inner propylitic alteration and no secondary biotite or orthoclase are present as indicators of potassic alteration zone, typical of most porphyry Cu settings. The minor Kfeldspar is interpreted as lower temperature adularia (photo 55). Minor epidote-magnetite-pyrite-chalcopyrite skarn with Au to 0.13ppm, Cu to 4467ppm and Mo to 98.3ppm, appeared to be less foliated than the adjacent rocks. Skarnoids may develop some distance from intrusion source rocks and so are not reliable indicators of the distance to a porphyry target. Folded epidote with axial planar sulphides provides a similar relationship between deformation and alteration suggested for Anomaly A.

Therefore, wall rock hydrothermal alteration intersected by DDH BTDD007 is indicative of a setting for this drill hole some distance from a targeted porphyry, and considerably further than Anomaly A west.

Some intensely deformed and altered intrusions host Au-Cu-Mo anomalism but are not overall significant (photo 59). Mineralised veins and shears and are mostly typical of those characterised as D veins formed marginal to porphyry intrusions are dominated by quartz-epidote-carbonate with pyrite-chalcopyrite (photos 57 & 60). Some porphyry style quartz-pyrite-chalcopyrite veins are present (photo 58) and a skarn is cited above. The local red sphalerite is typical of the interpreted setting some distance from a any intrusion source for this alteration and weak mineralisation.

CONCLUSIONS and RECOMMENDATIONS

Wall rocks intersected in drill core from the EW drill section in at Anomaly A host *out of porphyry* features (hydrothermal alteration and mineralised veins) typical of material commonly encountered near porphyry Cu deposits, and used as exploration vectors towards blind porphyry intrusion. Zoned hydrothermal alteration grades inwards as typical alteration shells (figure 2) as: chlorite -> epidote -> actinolite -biotite, regionally from cool in the east to hot conditions of formation at depth in the west. Cu mineralisation also varies from cooler deep epithermal to the east the higher temperature biotite-chalcopyrite assemblage in the west, becoming stronger at depth (photos 12, 17 & 18). In detail, the foliation has been active from ductile to later brittle condition as a strong structural control upon zoned alteration and mineralisation, localised in feeder structures that become stronger at depth to the west. Alteration and Cu mineralisation were initiated in conditions of ductile deformation (photos 18-20), and display a strong control by the penetrative foliation (photos 4, 12 & 22) including late reactivation in conditions of brittle deformation (photos 6 & 8). Syn-mineral uplift and erosion may have participated in this change from ductile to brittle conditions and

transient changes in the local stress regime re-opened the foliation to facilitate the introduction of additional sulphides.

There is no spatial or temporal correlation between Mo and Cu mineralisation which may be related to different intrusions. Mo mineralisation displays a strong relationship to phyllic altered intrusions, including post-deformation aplite dykes in DDH BT005. A typical quartz-molybdenite vein (photo 54) at extreme west of the Anomaly A data has been emplaced syn-deformation and may be indicative of a target in that vicinity. Cu and Mo may have been emplaced by different intrusions with Mo to be later than Cu mineralisation.

A target remains as the source for the zoned hydrothermal alteration and Cu mineralisation, down-dip from the hottest biotite-chalcopyrite assemblage, which would normally represent the wall rock alteration closest to a porphyry target (figures 2 & 3). However, this mineralisation such as the 33m @ 2045ppm Cu in the bottom of DDH DDBT010 already lies some 750m below the surface. The priority AB provided at this time, is indicative of a high priority but deep target, and may change with the increased understanding of the geological context (below). As the degree of dilation in the structures that transported mineralisation to the current setting remains unknown, it is difficult to estimate depth to target.

The entire Bottletree Project is provided with a priority A for a review that would apply this geological model to the entire area of interest in order to determine whether the current site of exploration is the best place to be working. All the individual prospects should be tabulated and prioritised for continued evaluation. This exercise will place the EW drill section in context in order to refine the target cited above.

Anomaly B wall rocks examined in one drill hole (DDH BTDD007) are dominated by epidote wall rock alteration typical of settings more distal to any porphyry source than the deep western portion of the EW drill section at Anomaly A (figures 2 & 3) and so is provided with a priority B-C for continued exploration at this time. This may change when this drill hole is placed in context.

Some age dates would represent a valuable addition to the Bottletree geological model.

References cited

Corbett, G.J., 2013, Pacific rim Epithermal Au-Ag: World Gold Conference Brisbane, Proceedings, Australasian Institute of Mining and Metallurgy, Publication Series 9/2013, p. 5-13.

Corbett, G.J., 2019, Time in porphyry Cu development – Exploration Implications: Pacrim Conference, 3-5 April 2019, Auckland, New Zealand, Australasian Institute of Mining and Metallurgy, p. 177-180.

Corbett, G.J., and Leach, T.M., 1998, Southwest Pacific gold-copper systems: Structure, alteration and mineralization: Society of Economic Geologists Special Publication 6, 238 p.

Dilles, J.H., Enaudi, M.T., Proffett, J., and Barton, M.D., 2000, Overview of the Yerrington Porphyry Copper District: Magmatic and nonmagmatic sources of hydrothermal fluids: Their flow paths and alteration effects on rocks and Cu-Mo-Fe-Au ores *in* Part I. Contrasting styles of intrusion-associated hydrothermal systems, Society of Economic Geologists Guidebook Series Vol 32, p. 55-66, Ed. T. B. Thompson.

Fournier, R.O., 1999, Hydrothermal processes related to movement of fluid from plastic into brittle rock in the magmatic-epithermal environment: Economic Geology 94, p.1193-1211.

Henderson R. A. and Withnall, I.W., 2013, Greenvale Province in Geology of Queensland Ed P.A. Bell, Queensland Government, p. 155-159.

Porter J.P., Schroeder, K., and Austin, G., 2012, Geology of the Bingham Canyon porphyry Cu-Mo-Au deposit, Utah: Economic Geology Special Publication 16, p. 127-146.

Seo, J.H., Guillong, M., and Heinrich, C.H., 2012, Separation of molybdenum and copper in porphyry deposits: The roles of sulphur, redox and pH in or mineral deposition at Bingham Canyon: Economic Geology, 107, p. 333-356.

Spencer, E.T., Wilkinson, J.J., Creaser, R.A., and Seguel, J., 2015, The distribution and timing of molybdenite mineralisation at the El Teniente Cu-Mo porphyry deposit, Chile: Economic Geology, 110, p. 387-421.

Tate, N., 2021, Bottletree Prospect, Summary Thoughts: unpubl. Memo.

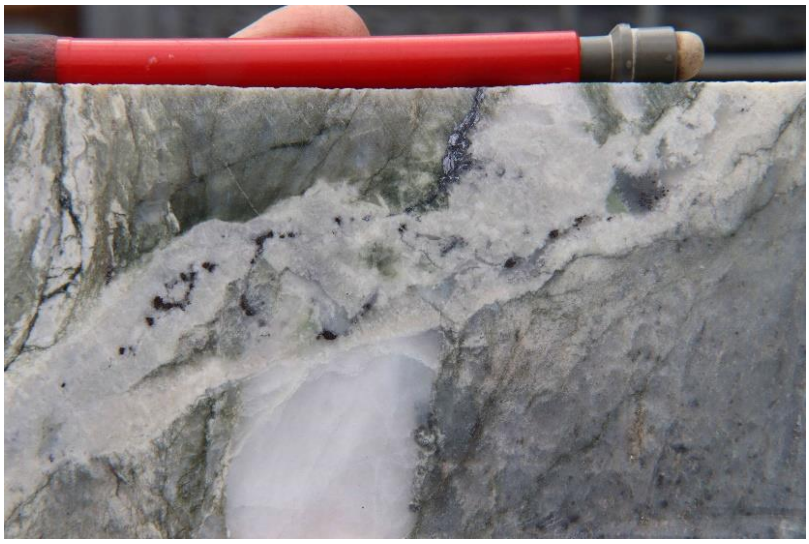

Photo 1 Aplite dyke with molybdenite cross cuts foliated wall rocks, DDH BTDD005, 510.7m.

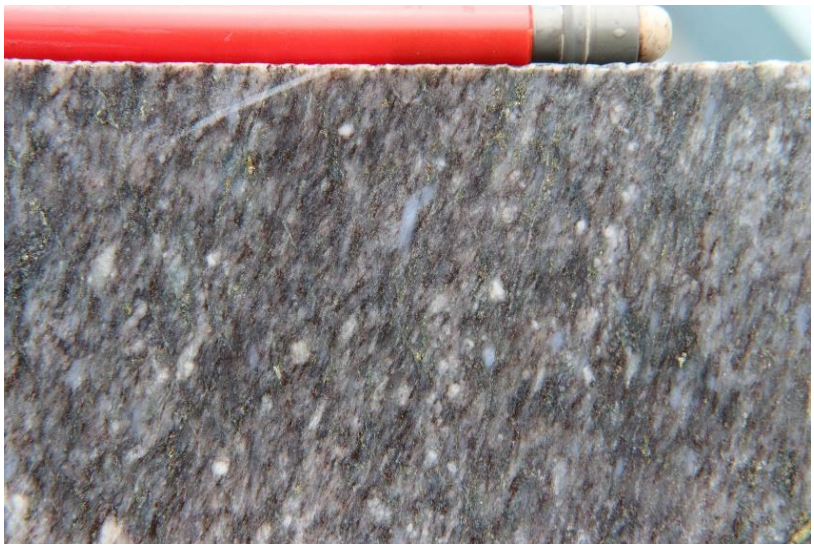

Photo 2 Biotite altered tonalite intrusion, DDH BTDD10, 581.9m.

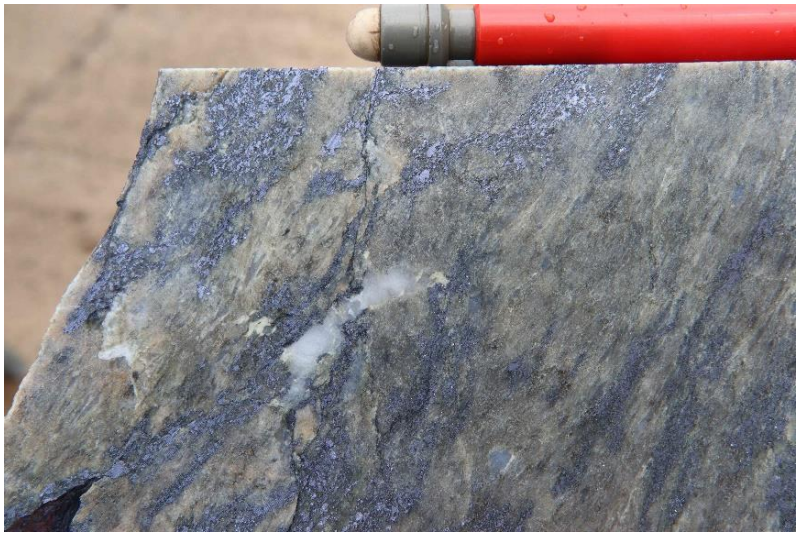

Photo 3 Intrusive dyke with intense sericite alteration and abundant molybdenite located at the dyke margin and within the Upper Mo Zone, DDH BTDD0010, 474m.

Photo 4 Penetrative foliation developed in a metavolcanic with silica-chlorite-actinolite alteration, DDH BTDD005, 566.3m.

Photo 5 Penetrative foliation developed in a tonalite with biotite and lesser epidote alteration, DDH BTDD004 625.7m.

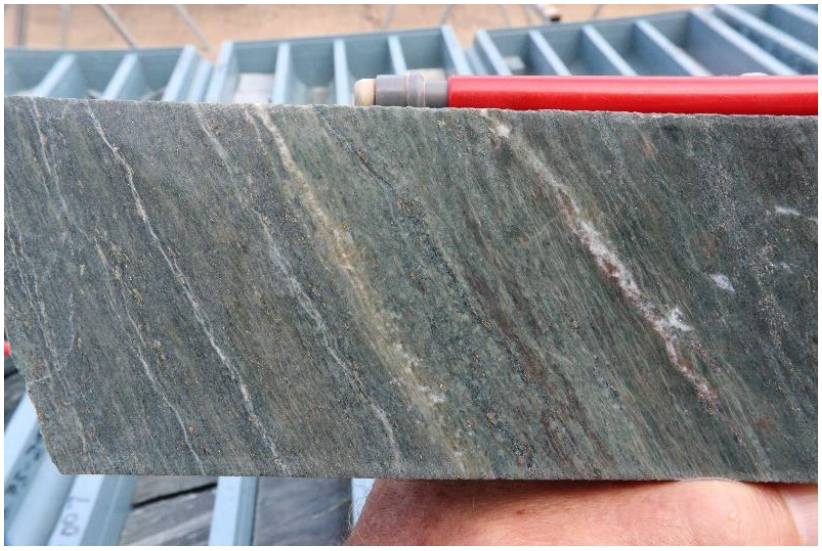

Photo 6 Intense foliation in silica-chlorite alteration, BTDD007, 300.8m.

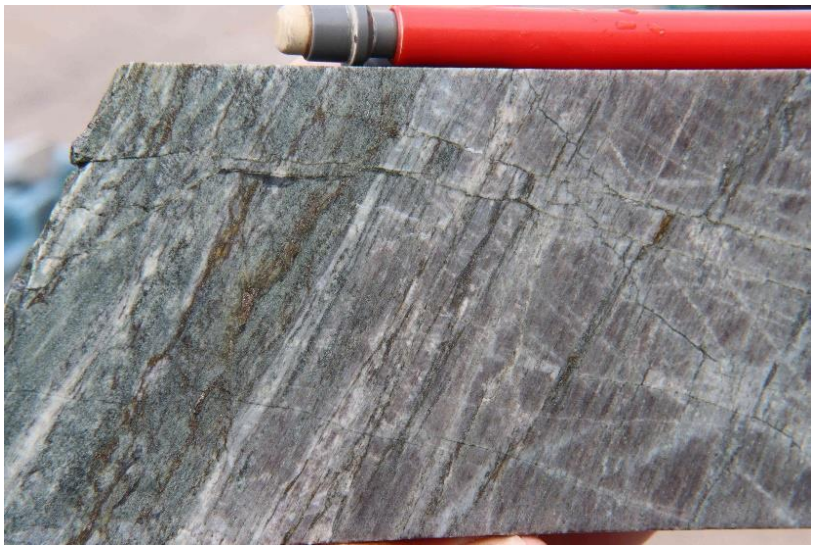

Photo 7 Strongly developed penetrative foliation with intense chlorite-silica alteration exploitation of partings by pyrite-chalcopyrite, DDH BTDD004, 530m, 0.37% Cu.

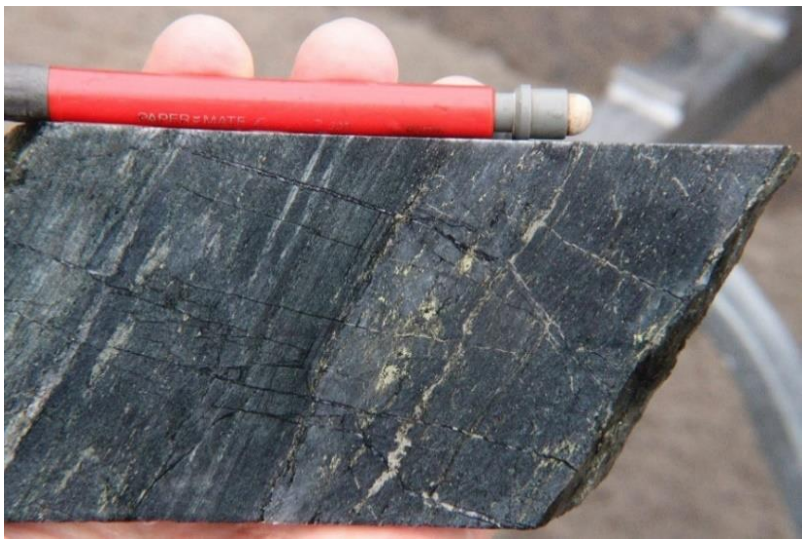

Photo 8 Strongly developed foliation with partings exploited by sulphides, some compositional layering and a ghosted fold on the left, DDH BTDD005. 661.3m. 3363ppm Cu.

Photo 9 Segregated foliation in chlorite-altered phyllite in which dismembered fold closures are discernible (as a syncline and anticline in the centre) DDH BTDD007, 493.3m.

Photo 10 Epidote cuts hornfels, DDH BTDD004 149.5m.

Photo 11 Pre-existing schistosity exploited by hydrothermal alteration characterised by silica-chlorite-actinolite, DDH BTDD005, 566.3m.

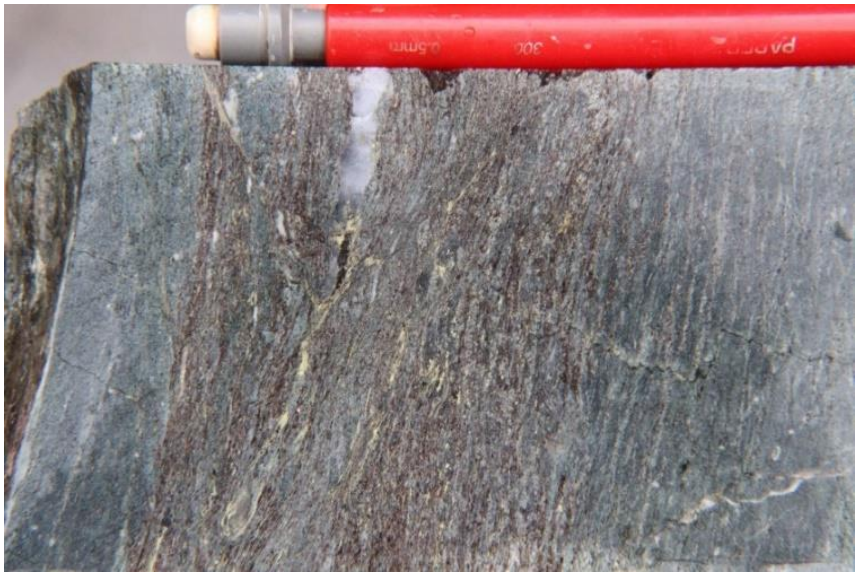

Photo 12 Foliated band of biotite-chalcopyrite cuts chlorite alteration, DDH BTDD005, 798.5m, 5121ppm Cu, 0.7ppm Mo.

Photo 13 Actinolite and biotite in foliation, DDH BTDD010, 1015.3m

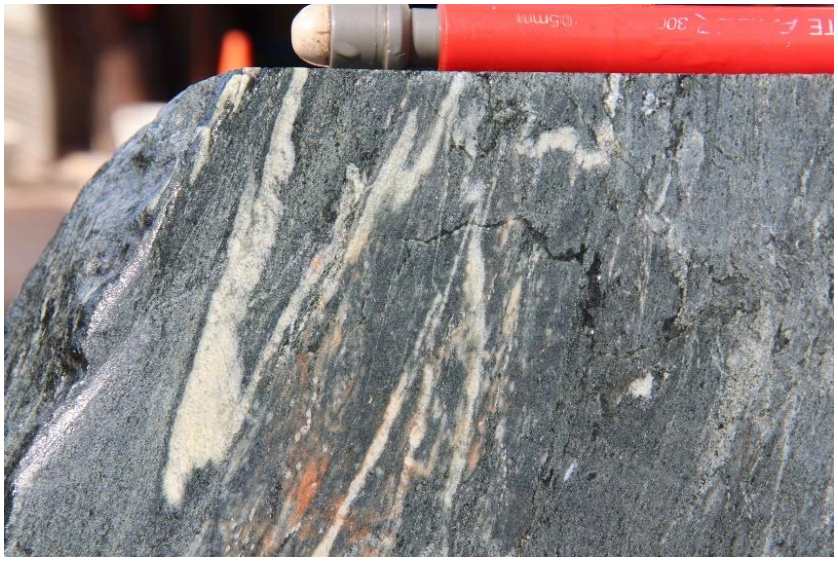

Photo 14 Folded epidote with the regional foliation as axial planar, DDH BTDD010, 843m.

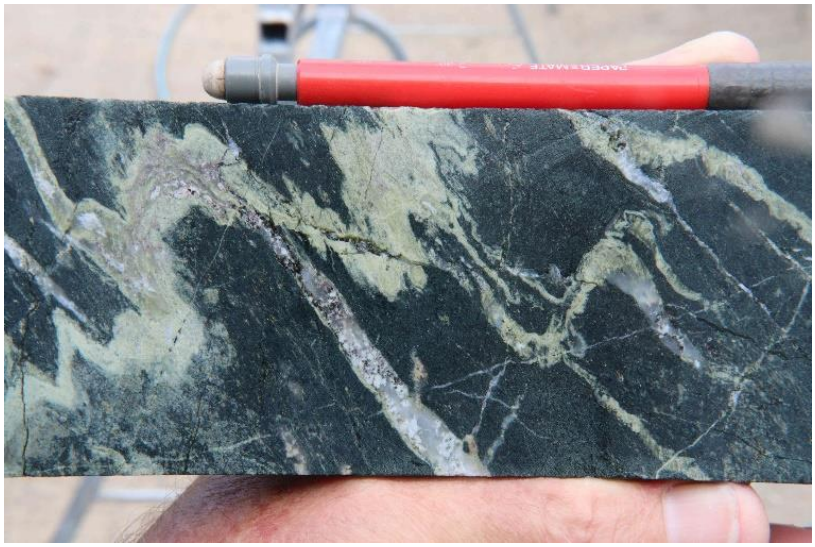

Photo 15 Folded epidote with the regional foliation as axial planar and a quartz-sulphide vein which both within the foliation and folded with the epidote, DDH BTDD007, 264.5m.

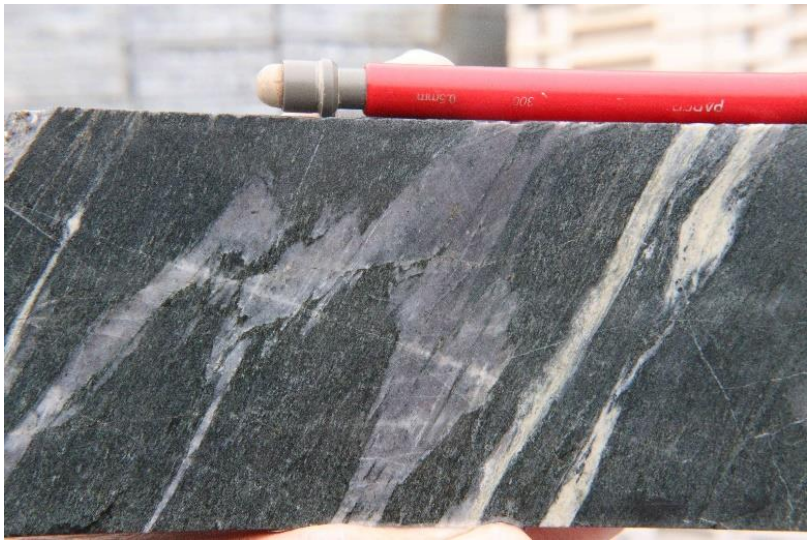

Photo 16 Early quartz (?A type) vein folded by compression associated with formation of the foliation which is exploited by epidote veins, DDH BTDD004, 162.1.

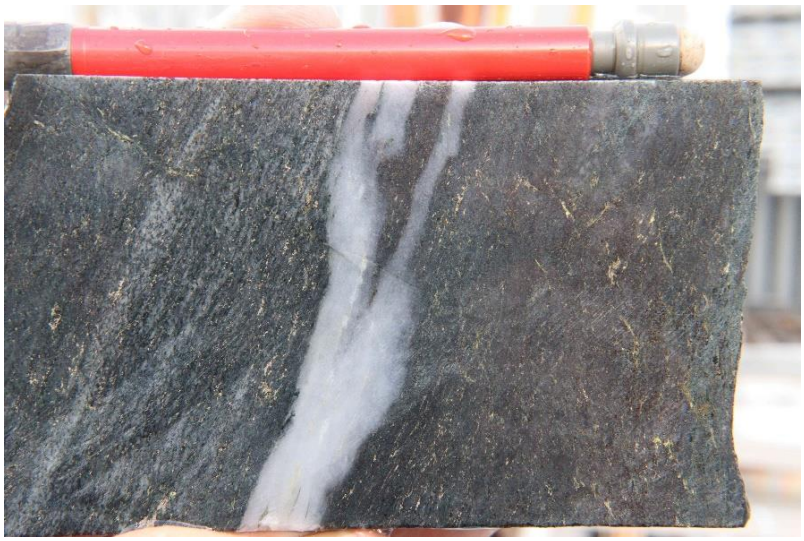

Photo 17 Zone of biotite-pyrite-chalcopyrite alteration within chlorite with sulphides as randomly oriented stringers, Bottletree DDH BTDD010, 676.6m, 537pm Cu.

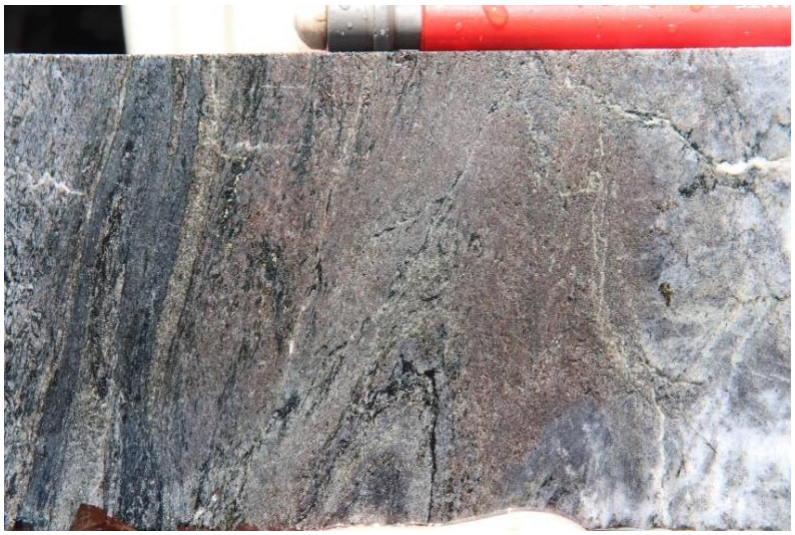

Photo 18 Tight-moderate folded biotite alteration on the right and near isoclinal folded chlorite on the left, DDH BTDD010, 912.3m.

Photo 19Folded epidote-actinolite-biotite alteration, DDH BTDD010, 229.1m.

Photo 20 Fold with incipient development of axial planar epidote-actinolite, DDH BTDD004 621.4m.

Photo 21 Biotite both cross cuts and is within foliation, DDH BTDD010, 929.1m.

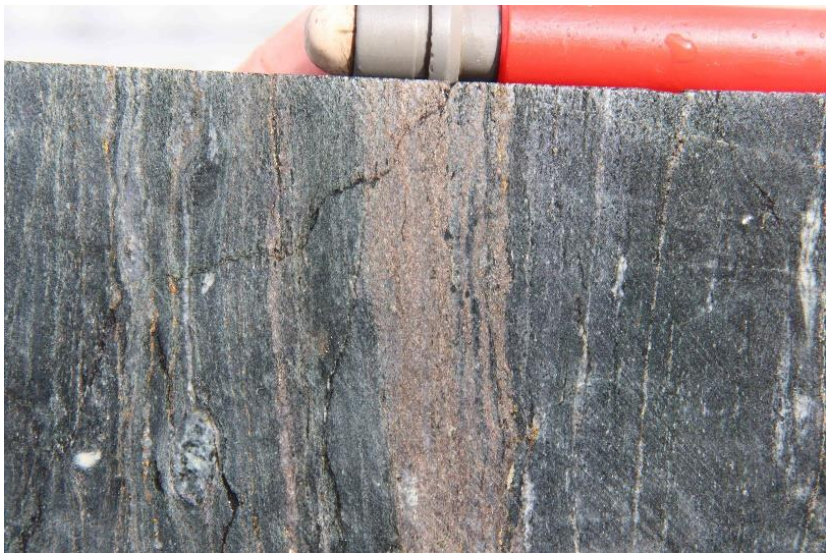

Photo 22 Intensely foliated chlorite altered metavolcanic in which the foliation is locally exploited by biotite alteration and elsewhere by chalcopyrite, DDH BTDD004, 302m 0.46% Cu.

Photo 23 Feldspar porphyry dyke with actinolite alteration emplaced parallel to foliation, DDH BTDD004, 142m.

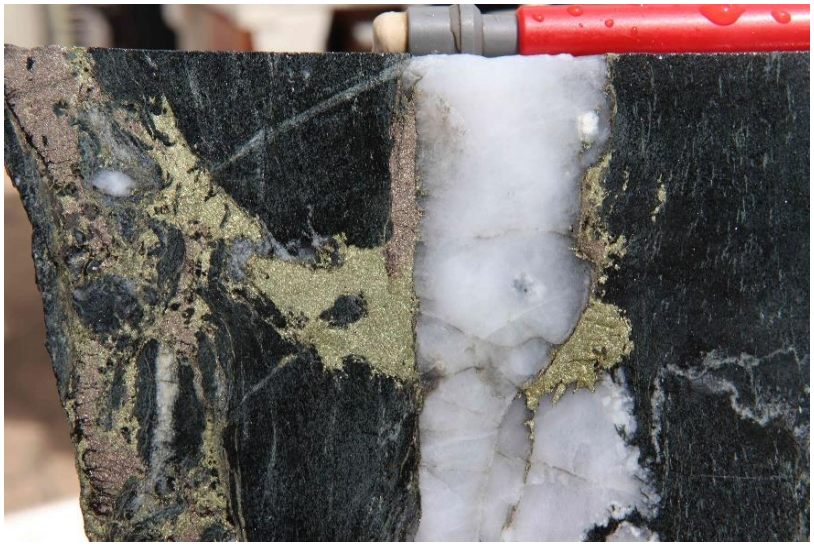

Photo 24 Quartz-pyrite-pyrrhotite vein initiated within foliation but also cutting it DDH BTDD005, 727.1m,0.71% Cu.

Photo 25 Quartz-chalcopyrite vein parallel to foliation in chlorite-actinolite schist, DDH BTDD005, 687.4m, 0.11% Cu.

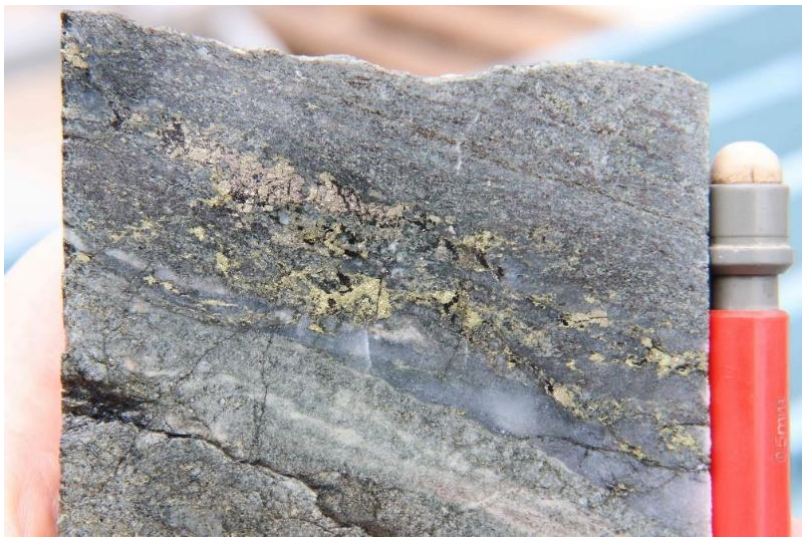

Photo 26 Quartz-pyrite-chalcopyrite vein with sericite overprint within the trend of foliation, DDH BTDD010 908.9m, 0.38% Cu.

Photo 27 Biotite wirh silica-chlorite alteration overprint in foliation parallel shear-hosted quartz-chalcopyrite-pyrrhotite, DDH BTDD010, 903.5m, 0.51% Cu.

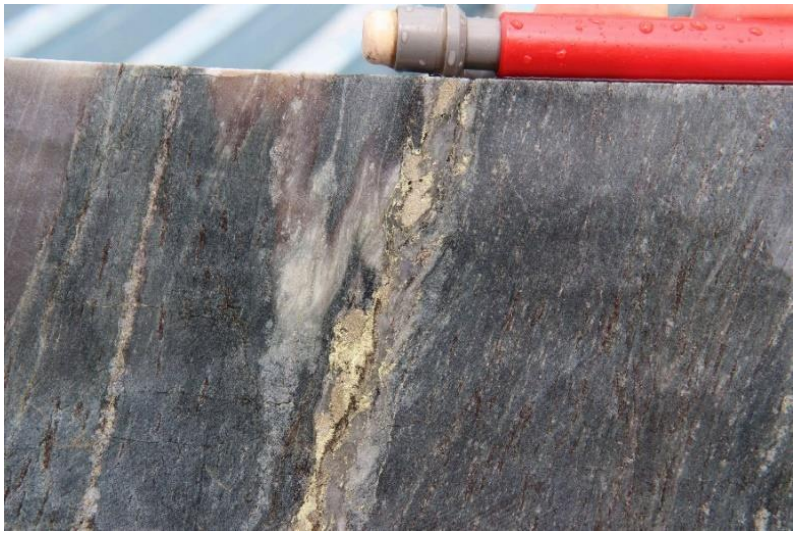

Photo 28 Strongly foliated rock with biotite in the foliation cut by pyrite-chalcopyrite vein with sericite-chlorite selvage, BTDD010, 1007m.1, 0.3% Cu.

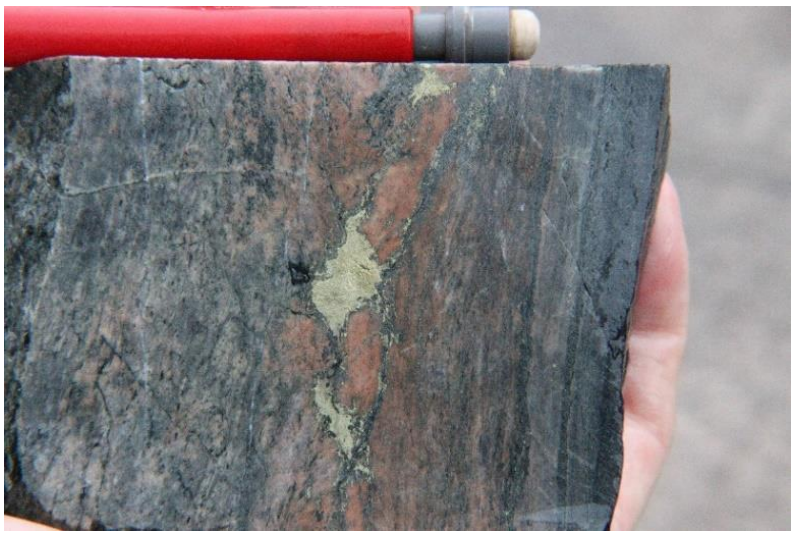

Photo29 Foliation exploited by chalcopyrite-Kfeldspar-actinolite, DDH BTDD005, 584.4m, 0.33% Cu.

Photo 30 Foliation parallel zone of biotite-pyrite-chalcopyrite alteration within chlorite, and with a later D vein at the RH margin, DDH BTDD010, 898.1m, 0.27% Cu.

Photo31 Quartz-biotite-chalcopyrite shear parallel to foliation, DDH BTDD004, 281.9m, 0.17% Cu.

Photo 32 Foliation parallel to the core axis that terminated at cross structures in a sigmoid shape, DDH SBTRD006, 368.1m 0.63% Cu, 0.8% Cu.

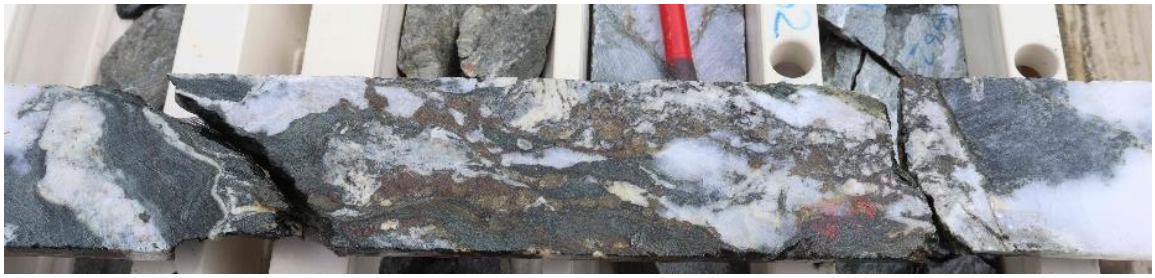

Photo 33 Mineralised quartz-sulphide vein parallel to the core axis that terminates at two cross structures in a sigmoid shape, DDH SBTRD006, 361.5m, 0.63%.

Photo 34 Foliation and a quartz-chalcopyrite-pyrrhotite both at a low angle to the core axis DDH BTDD004, 367.7m, 0.16 g/t Au & 2.00% Cu.

Photo 35, Quartz-chalcopyrite-pyrrhotite vein aligned within the foliation at a modest angle to the core axis, DDH BT004, 598.1m, 0.13% Cu.

Photo 36 Pyrite-chalcopyrite mineralisation within sericite overprint within a fault with 0.12ppm Au and 0.6% Cu, similar to deep low sulphidation quartz-sulphide Au $\pm$ Cu mineralisation, DDH BTDD4, 524.9m, 0.12ppm Au, 0.61% Cu, 3ppm Mo.

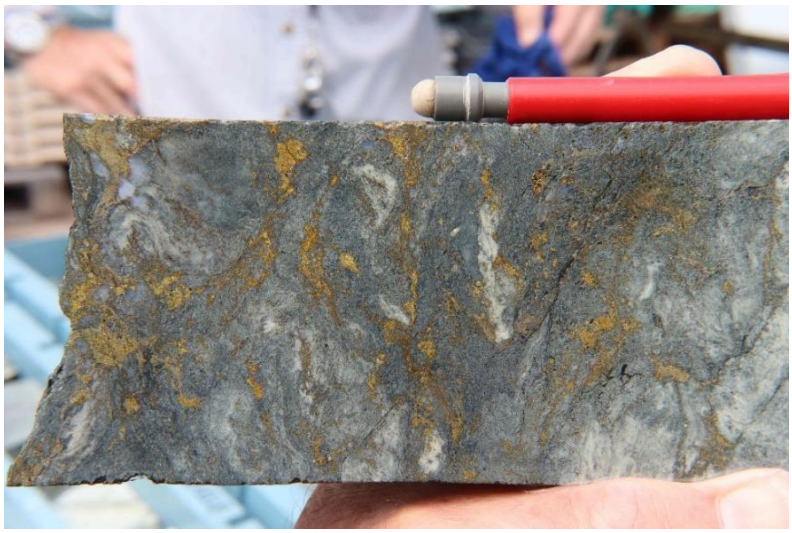

Photo 37 Chalcopyrite within complexly folded foliation in the footwall fault zone, DDH DTDD004, 632.3m 0.23ppm Au & 1.97% Cu, as part of 6m @ 0.8% Cu.

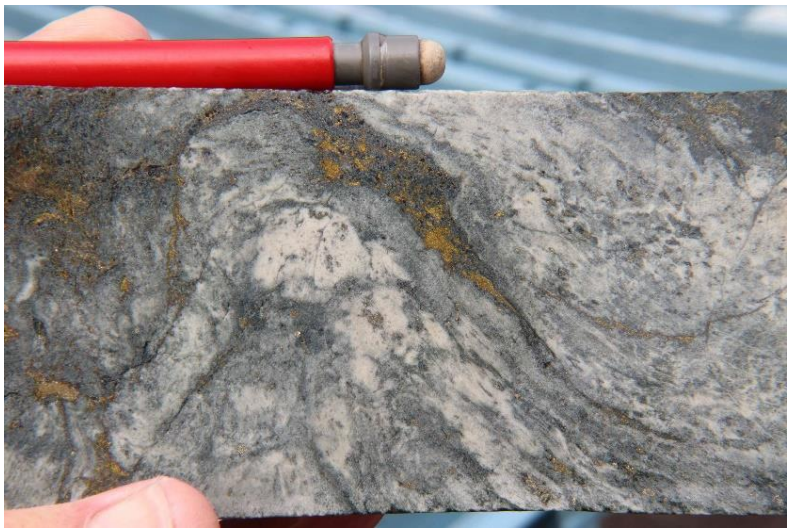

Photo 38 Chalcopyrite within folded foliation adjacent to fault, DDH DTDD004, 632.7m 0.23ppm Au & 1.97% Cu, as part of 6m @ 0.8% Cu.

Photo 39 Quartz-chalcopyrite exploits foliation near fault 0.1ppm BTDD004, 637.3m, 0.1ppm Au & 0.48% Cu, as part of 6m @ 0.8% Cu.

Photo 40 Molybdenite stringer within a phyllic altered tonalite dyke in the Upper Mo Zone, DDH DTDD005, 483.3m, 103ppm Cu & 962ppm Mo.

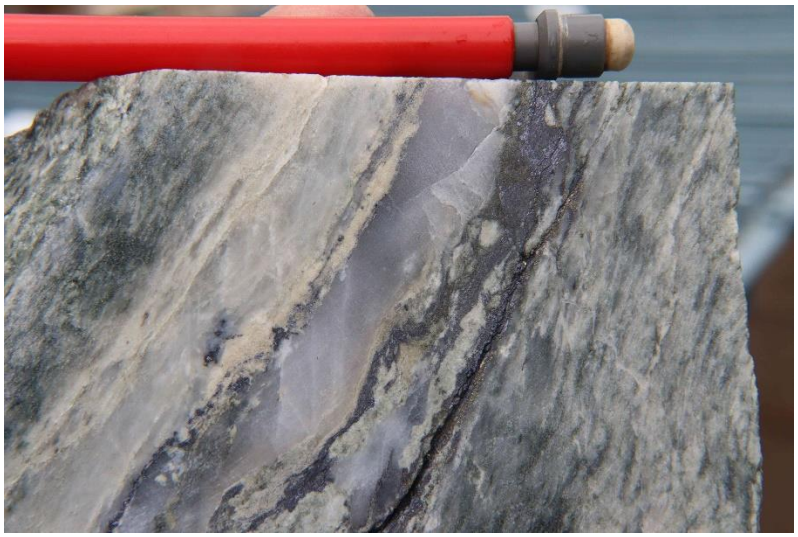

Photo 41 Foliation-parallel quartz-molybdenite vein with sericite selvage likened to D vein, DDH BTDD005, 486.3m, 1386ppm Mo & 73ppm Cu.

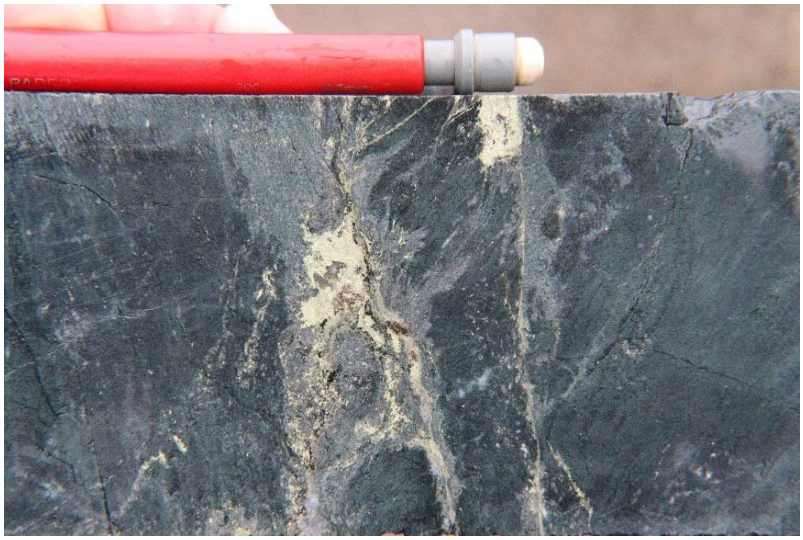

Photo 42 Chalcopyrite shear cuts and offsets silicified foliation. DDH BT005, 720.2m, 0.6% Cu, 1.7ppm Mo.

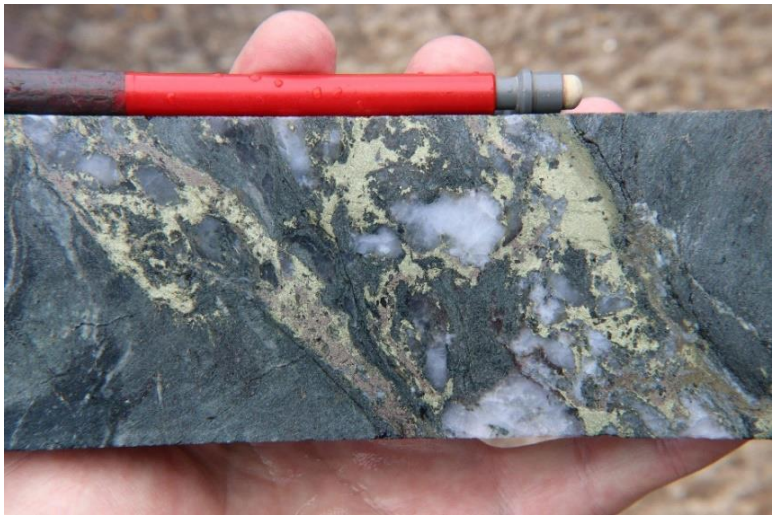

Photo 43 D vein characterised by quartz-chalcopyrite-pyrrhotite and yellow-red sphalerite cross-cuts and folds chlorite, BTDD005, 748.3m, 0.12% Cu, 1.2ppm Mo.

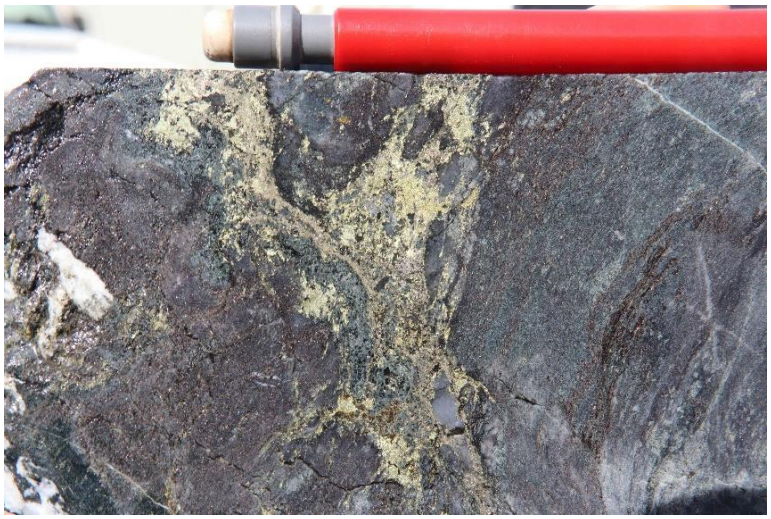

Photo 44 Biotite-pyrrhotite-chalcopyrite with biotite-actinolite selvage alteration cuts chlorite alteration, DDH BTDD010, 888.4m, 0.62% Cu & 1.9ppm Mo.

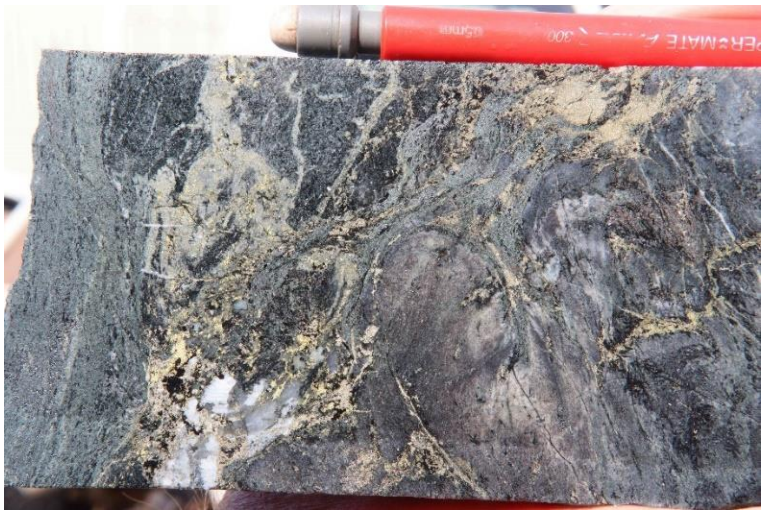

Photo 45 Chlorite alteration cut by biotite-pyrite-chalcopyrite-pyrrhotite with actinolite selvage, BTDD010, 890.4m, 0.21% Cu & 2.1ppm Mo.

Photo 46 Quartz-molybdenite hosted within chlorite-sericite shear, DDH BTDD010, 675.6m 157ppm Cu & 14ppm Mo.

Photo 47 Strongly foliated rock with pyrrhotite (LHS) and a D vein with pyrite-chalcopyrite possible bornite (RHS) and minor secondary biotite with sericite overprint, DDH BTDD010, 1022.8m, 0.19% Cu & 2.7ppm Mo.

Photo 48 Actinolite aligned within the foliation with probable white albite, DDH BTDD005, 558.7m.

Photo 49 Massive actinolite, DDH BTDD005, 598.3m.

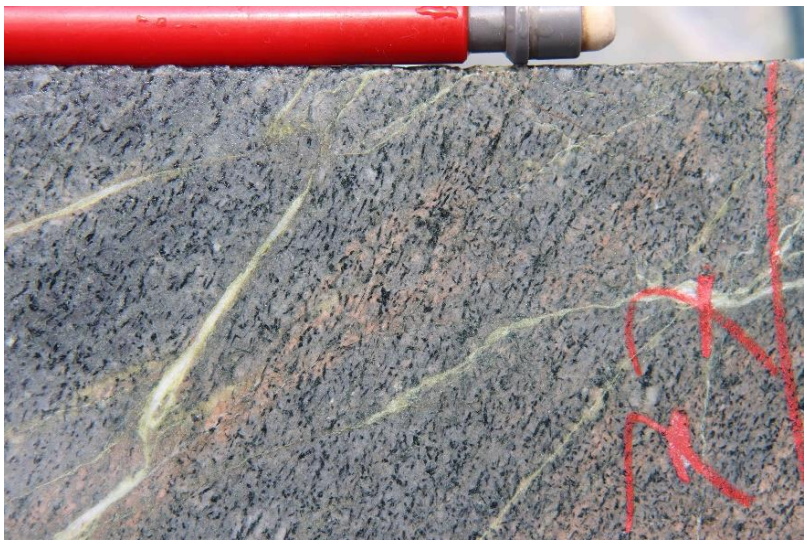

Photo 50 Actinolite partly aligned within the foliation with pink adularia, DDH BTDD010, 77m.

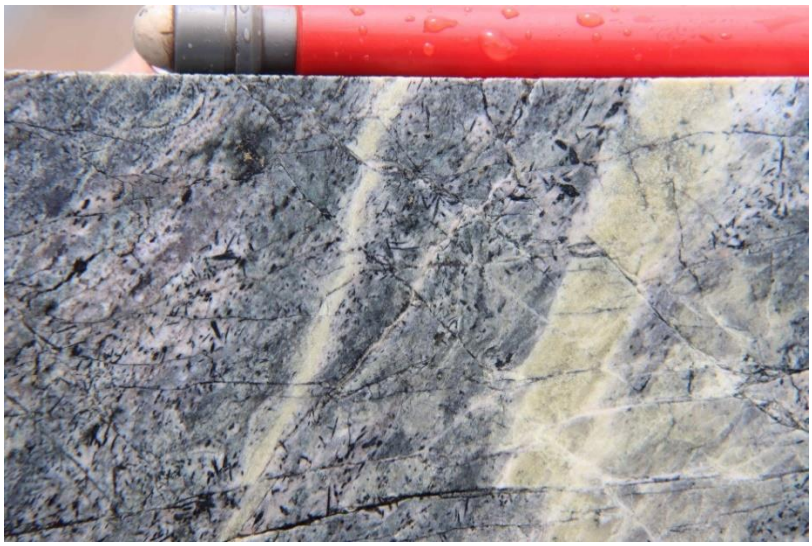

Photo 51 Actinolite-epidote aligned within the foliation, DDH BTDD010, 65.3m.

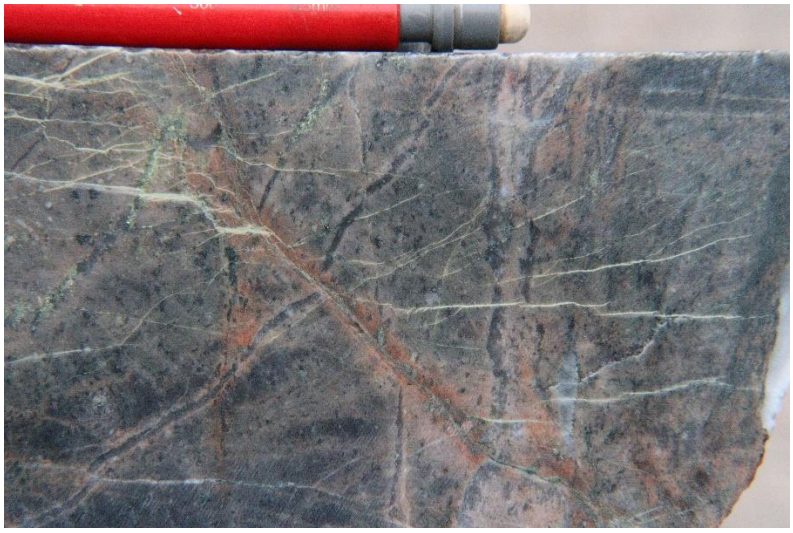

Photo 52 Silica-chlorite alteration cut by quartz veinlets with Kfeldspar (adularia or orthoclase) selvages, DDH BTDD005, 576.1m.

Photo 53 Silica-chlorite alteration with foliation-parallel quartz veins with Kfeldspar (adularia or orthoclase) selvages, DDH BTDD005, 639.4m.

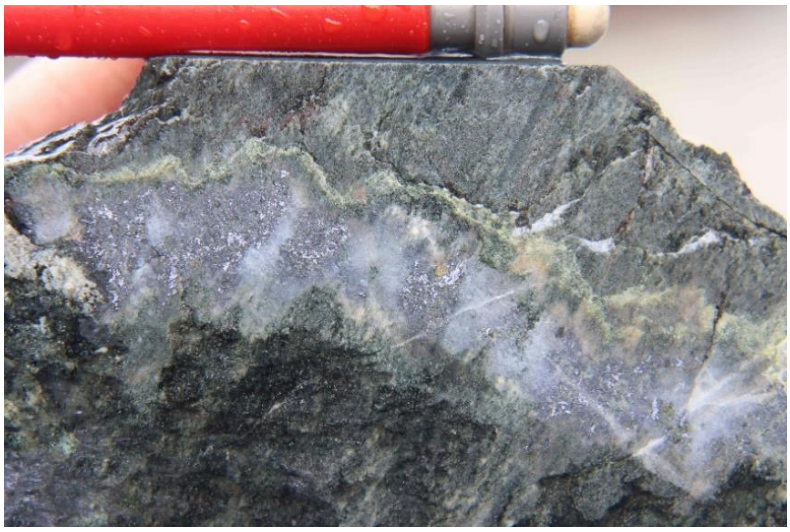

Photo 54. Syn-deformation(cuts foliation and is cut by it) porphyry-style quartz-molybdenite vein with prograde epidote selvage. DDH BTDD010, 252.5m.

Photo 55 Foliated silica-chlorite-adularia alteration with sulphide in the foliation, DDH DTDD007, 318.7m.

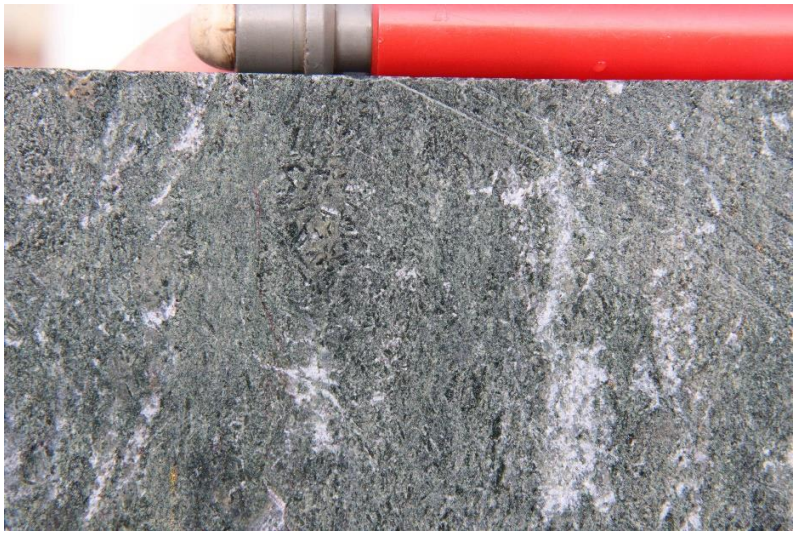

Photo 56 Chlorite-carbonate-actinolite, DDH BTDD005, 261m.

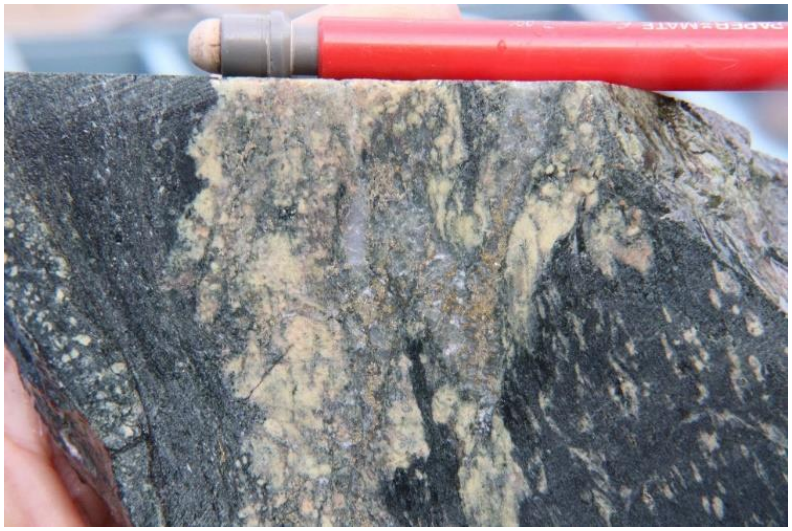

Photo 57 Epidote alteration with quartz-pyrite chalcopyrite mineralisation DDH BTDD005, 285.4m, 702ppm Cu & 1.4ppm Mo.

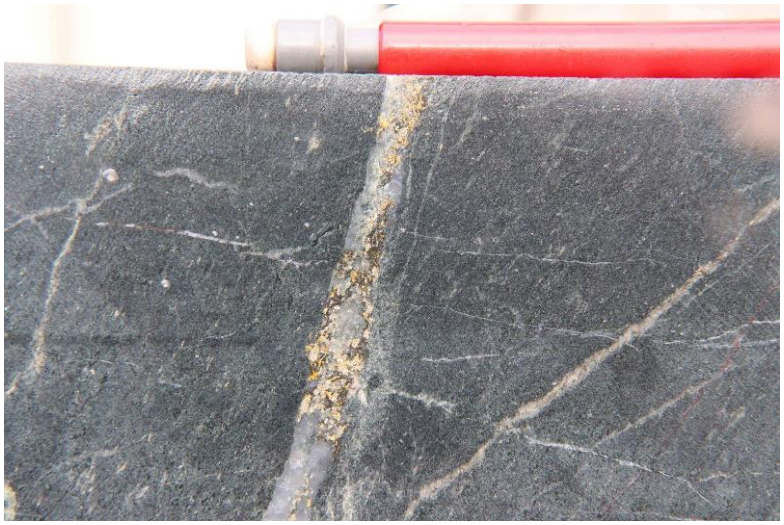

Photo 58 Possible porphyry A vein characterised by quartz-pyrite-chalcopyrite within chlorite altered wall rock, DDH BTDD005, 283.4m, 616ppm Cu, 1.1ppm Mo & no significant Au.

Photo 59 Sheared and intensely sericite altered intrusion, DDH BT007, 191.3m, 943ppm Cu, 1.2ppm Mo & 0.22ppm Au.

Photo 60 Shear with quartz-chlorite-carbonate-epidote-pyrite-chalcopyrite, DDH BTDD007, 268.7m, 835ppm